THE EFFECT OF HEIGHT ON BONE STRAIN WHILE PERFORMING DROP LANDINGS

A THESIS SUBMITTED TO THE GRADUATE SCHOOL IN PARTIAL FULFILLMENT OF THE REQUIREMENTS FOR THE DEGREE

MASTER OF SCIENCE

BY

SCOTT S. DUEBALL

ADVISOR: DR. ERIC DUGAN

BIOMECHANICS LABORATORY

BALL STATE UNIVERSITY

MUNCIE, INDIANA, USA

July 2010

THE EFFECT OF HEIGHT ON BONE STRAIN WHILE PERFORMING DROP LANDINGS

A THESIS SUBMITTED TO THE GRADUATE SCHOOL IN PARTIAL

FULFILLMENT OF THE REQUIREMENTS FOR THE DEGREE

MASTER OF EXERCISE SCIENCE

BY

SCOTT S. DUEBALL

COMMITTEE APPROVAL:

Committee Chairperson (Dr. Eric L. Dugan)	Date
Committee Member (Dr. He Wang)	Date
Committee Member (Dr. Lisa Jutte)	Date

DEPARTMENTAL APPROVAL:

Graduate Coordinator	Date

GRADUATE OFFICE CHECK:

Dean of Graduate School	Date

BALL STATE UNIVERSITY

MUNCIE, INDIANA, USA

August 10

DECLARATION

The work presented in this thesis is, to the best of my knowledge and belief, original, except as acknowledged in the text, and the material has not been submitted, either in whole or in part, for a degree at this or any other university.

_____

Scott Steven Dueball

ACKNOWLEDGMENTS

First and foremost, thanks to the Great Architect of the Universe for his continued guidance, forgiveness, and support in the many aspects of my life.

Thanks to the love of my life, Rosalee, for her unending encouragement and understanding. This is for us.

Kate, without whom this project would not have been completed. Thank you for your time, support, and most of all friendship.

My family to whom I owe gratitude for the many opportunities that they have given me. My father, who has been there every step of the way, has been my guide through this project and in life. My mother who continually picks me up and puts me back on my feet when I fall. Twinkie for being there when I needed someone and for her help in editing this paper. Heggie for being my best friend even when I'm difficult.

Tameka, I learned so much from assisting you. The things that you taught me through your thesis really helped to stay motivated through the rough spots of research. I cannot thank you enough.

Dan Leib who responded to countless emails and phone calls with questions regarding the modeling procedure. Dan and Scott Bergeon are primarily responsible for the design of the process outlined herein. Future research in modeling will be indebted to them.

My thesis committee, Eric Dugan, Lisa Jutte, and Henry Wang, who helped develop my research and writing skills throughout this process.

Lisa Kaufman, who was always there to help when things were stressful. The Lab would be a disaster without her.

This project was made possible through the support of the Ball State Sponsored Program Office and their ASPiRE internal grant.

I would also like to thank Sherry Simmonds and the imaging staff at Ball Memorial Hospital who worked with me whenever they could squeeze our subjects in.

Finally, I would like to thank Mrs. (Barb) Lightfoot whose lesson made such a difference in my life. I am only beginning to see her affect on me. I owe her many thanks.

ABSTRACT

THESIS: The Effect of Height on Musculoskeletal Injury While Performing Drop Landings

STUDENT: Scott S. Dueball

DEGREE: Master of Science

DATE: August 10

PAGES: 101

During landing, the human body is required to absorb impact forces throughout its tissues. Muscle and connective tissue is able to dissipate much of this force. However, a portion of the impact is delivered to the bones. Forces entering the human skeleton can cause microscopic fractures which may lead to stress fracture. The present study seeks to evaluate changes in the magnitude of strain using noninvasive methods. A musculoskeletal model representing a healthy male subject (22 years, 78.6 kg, 1.85 m) was created. A flexible tibia, created from a computed tomography scan of the subject's right tibia, was included in the model. Motion capture data were collected while the subject performed drop landings from three separate heights (26, 39, and 52 cm) and used to compute simulations in LifeMOD. Surface electromyography and joint angle data were compared to their simulated counterparts using a cross correlation to the model. Maximum magnitudes of principal and maximum shear strain were computed. The model had reasonable agreement between joint angle curves and muscle activation patterns. A large Cohen's d effect size showed that our subject had increased tibial strain and strain rate as the drop height increased. This study demonstrates a valid method of

simulating tibial strain. Future studies should focus on recruiting a larger sample and applying the model.

TABLE OF CONTENTS

COMMITTEE APPROVAL: ii
DECLARATION iii
ACKNOWLEDGMENTS iv
ABSTRACT v
TABLE OF CONTENTS vii
LIST OF TABLES ix
LIST OF FIGURES x
NOMENCLATURE xi
DEVELOPMENT OF THE PROBLEM 13
INTRODUCTION 13
PURPOSE 14
SIGNIFICANCE 15
METHODS 15
LIMITATIONS 17
DELIMITATIONS 17
SUMMARY 17
REVIEW OF LITERATURE 19
INTRODUCTION 19
Incidence of Stress Fracture in the Tibia 20
Etiology of Stress Fractures particularly in the Tibia 22
Common Stress Fracture Sites 24
Landing Activities and Stress Fractures 25
Muscular Strength and Stress Fracture 26
Improvements in Methods of Studying Bone Strain 29
Potential Drawbacks to FEA 31
PID Controllers and Musculoskeletal Simulation 31

Adding Muscle to the Model 34
Summary 36
METHODS 37
INTRODUCTION 37
EXPERIMENTAL PROCEDURE 38
Subject Description 38
Experimental Overview 38
Data Collection 40
Overview of Modeling Procedure 43
MODEL DESIGN 44
Flexible Tibia Creation 44
Musculoskeletal Model Creation 46
DATA MANAGEMENT 47
Data Processing 47
Data Analysis 49
RESEARCH ARTICLE 51
ABSTRACT 53
INTRODUCTION 54
METHODS 56
RESULTS 61
DISCUSSION 63
CONCLUSIONS 67
SUMMARY AND CONCLUSIONS 84
SUMMARY 84
CONCLUSIONS 85
RECOMMENDATIONS FOR FUTURE RESEARCH 88
REFERENCES 89
Informed Consent 95
Software Descriptions 100

LIST OF TABLES

Table 1- Cross Correlation Coefficients between collected and modeled muscles

Table 2- Previous Tibial Strain Research

Tables from Chapter 4

Table 1- Cross Correlation Coefficients between joint angles

Table 2- Cross Correlation Coefficients between muscle forces and EMG

Table 3- Tibial Strain and Strain Rate derived from LifeMOD

Table 4- Cohen's d Effect Size comparing tibial deformation among drop heights

LIST OF FIGURES

Figure 1- Diagram of muscle forces in the leg

Figure 2-Graphical explanation of PID control

Figure 3- Example reflective markers and marker clusters

Figures from Chapter 4

Figure 1- Musculoskeletal model used in the study

Figure 2- Angle comparisons between Visual 3D and LifeMOD in one 26cm trial

Figure 3- Angle comparisons between Visual 3D and LifeMOD in one 39cm trial

Figure 4- Angle comparisons between Visual 3D and LifeMOD in one 52cm trial

Figure 5- Muscle activation comparison for one 26cm trial

Figure 6- Muscle activation comparison for one 39cm trial

Figure 7- Muscle activation comparison for one 52cm trial

Figure 8- Strain produced from landing heights

Figure 9- Strain rate produced from landing heights

NOMENCLATURE

ASIS-Anterior Superior Iliac Spine

Craig Bampton- Method of simplifying the finite element analysis by solving deformation modes at various vibration frequencies.

CT Scan- Computed Tomography- A common method of medical imaging.

EMG-Electromyography- Uses skin surface sensors to detect muscle activation levels.

FEA-Finite Element Analysis- A technique commonly used in engineering to estimate solutions to complex numerical problems. Bodies are broken down into a finite number of nodes. Forces can be applied to the body and software can calculate the resulting nodal movement.

FEM-Finite Element Mesh- Model created for use in the FEA.

GeBOD-Generator of Body Data- A database of segment (limb) properties used by LifeMOD.

Gravitational Potential Energy-The energy a body has while at rest as a result of Earth's gravitational pull. $\Delta U = mg\Delta h$, where m is the mass of a body, g is the gravitational acceleration applied on the body, and h is the height of the body.

Inverse Kinematic Simulation-The first step in the modeling process where the kinematics are used to record the muscle length/time curves.

LifeMOD-A multi-body dynamic modeling software used to simulate movement.

M-file- Computer scripts written in Matlab.

MNF-Modal Neurtal File- A file containing an objects mass, stiffness, modal response information.

Node- The intersection of element perimeters about which values are calculated.

Normalize-The ability to compare data between subjects commonly down by dividing a value by body mass or maximal contraction.

Osteoblasts- Cells that break down bone.

Osteoclasts- Cells that form bone.

Plantarflexors- The group of muscles that cause the ankle to plantarflex or point your toes.

PID Control-Proportional-Integral-Derivative- A method of control used in industry which contains a three-term weighted sum of errors.

Strain-The deformation a body experiences. The movement of a body's particles is represented by the strain. Measured in units of microstrain (10^{-6}). $e = \frac{\ell - L}{L} = \frac{\Delta L}{L}$. Principal strain is measured along the three principal axis.

Subject Specific-Method of creating a model for a specific person versus a model that describes a general sample.

TSF-Tibial stress fracture

Yield Strength- The point at which a material will deform plastically or permanently. Typically, this refers to the limit of load that can be applied.

Young's Modulus- The measure of stiffness of an isotropic material.

CHAPTER 1

DEVELOPMENT OF THE PROBLEM

INTRODUCTION

Landing from a jump is an essential movement performed both in sport and military activities [1]. During landing, the body experiences impact forces which must be dissipated throughout the tissues of the body. Much of this impact is dissipated mechanically through muscle and connective tissues [2, 3]. However, some portion of the landing force is absorbed by hard tissue such as bone.

Bone is exposed to ground reaction, inertial, and muscular forces. Ground reaction forces cause large forward bending in the tibia while posterior musculature works to resist this action [4]. Local deformation occurs when muscle forces act at small

attachment points [5]. Forces entering the bone result in deformation. The remodeling process begins as a result of deformation [6]. During remodeling, bone is weakened as damaged tissue is removed leaving cavities [7]. Without proper rest, bone will remain in the weakened state allowing fractures to form.

Applied forces may be acute and high in magnitude or chronic and low in magnitude. These chronic, low magnitude forces are well below the yield strength of bone [8], however they are still capable of causing microdamage through cyclical loading from[6]. As microdamage accumulates in the absence of proper rest, fracture can occur [9]. Failure of this type is referred to as a stress fracture.

Athletes and military recruits are at risk of accumulating microdamage that can result in fracture because of the rapid increase in intensity or new training regimens combined with a lack of rest which is common to their training [9, 10]. Bone can adapt to these changes in exercise but without adequate rest cavities form which eventually turn into fracture. It is important to understand the bone deformation caused by human movement in order to develop stress fracture prevention strategies. A better understanding of the injury can be gained by examining the tibial strain and strain rates during various exercises.

PURPOSE

The purpose of this study is twofold. The primary purpose of this study is to develop a non-invasive musculoskeletal modeling technique for use in drop landing. The secondary goal is to obtain tibial strain and strain rate values from the model.

SIGNIFICANCE

Documenting changes in tibial strain during drop landings will further our understanding of how different activities may lead to the development of stress fractures. Researchers have sought to use computer simulation to evaluate strain and strain rates in bone as a non-invasive alternative to *in-vivo* research methods [2]. Simulation methods have not been used to examine strain in drop landing. By applying the simulation approach it may be possible to examine bone deformation in larger cohorts in future research. The addition of subject specific bone geometry when creating the flexible tibia model will improve upon the usefulness of previous methods as well.

METHODS

One 22 year old male subject volunteered for this study. The subject had a mass of 79 kg and was 1.85 m tall. The subject was required to have a tibial CT scan within the past four months. To evaluate changes in strain and strain rate while landing, the subject performed drop landings from three different heights. The independent variable is the drop height. The three heights were set at 26, 39, and 52 cm. The subject was instructed in how to step off the box but not in landing technique specifically. The subject was instructed to land and remain standing until the research team completed capturing the trial. The dependent variables, peak strain and strain rate, were extracted from the analysis. Three landings were performed from each height in order to calculate averages in the dependant variables.

A 14-camera Vicon F Series (Vicon, Oxford, UK) motion capture system collected the motion data during the drop landings. A cluster based marker set was chosen for this study. Clusters were attached to the subject's ASIS, thigh, and shank on

both sides. The Plug-in-Gait (Vicon Oxford, UK) bony landmarks used were the posterior superior iliac spine (PSIS), lateral knee femoral epicondyle, lateral malleolus, calcaneous, toe, and first metatarsal joint. In addition to the Plug-in-Gait (PiG) landmarks, markers were attached to the medial knee femoral epicondyle, medial malleolus, and fifth metatarsal. A pelvic crest marker was attached to a Velcro patch on the shorts. Muscle activity was recorded using a 16-channel Bagnoli Desktop EMG (Delsys Inc., Boston, MA). Surface EMG electrodes captured the activity of the vastus medialis, vastus lateralis, medial hamstring, medial gastrocnemius, tibialis anterior, and the soleus in both legs. Ground reaction forces were collected using two AMTI multi-axis force platforms (Advanced Mechanical Technology, INC. Watertown, MA).

The kinetic and kinematic data were processed using both Vicon Workstation (Vicon Oxford, UK) and Visual 3D (C-Motion, Germantown, MD) software packages. Markers were labeled and the trials were cropped in Workstation. Visual 3D was used to filter kinetic and kinematic data. Processed data was exported from Visual 3D and converted to a format readable by LifeMOD (BRG, San Clemente, CA). The processed data was used to create a lower-body, musculoskeletal model of the subject performing the landing. The CT scan of the tibiae was used to create a 3-dimensional finite element mesh (FEM) to be inserted into the musculoskeletal model. Customized modeling software allowed the tibiae FEM to be tested under simulated loads. The strain and strain rate values were extracted from this simulation.

The model needs to represent the actual motion as close as possible. To verify this, kinematic and surface EMG data were recorded and compared. Cross correlations were used to compare the Visual 3D joint angles and EMG activity to the LifeMOD joint

angles and muscle forces. The modeled strain values were calculated. A Cohen's d effect size was used to compare the strain data from the three different landing heights.

LIMITATIONS

The subject used in this study was given minimal instruction on how to land in order to examine the most natural movement possible. The strain results obtained from this study will represent this subject specifically and not a larger sample or population. The subject performed the motion without shoes. Being barefoot undoubtedly affects the kinematics of drop landing. The musculoskeletal model was developed for the purpose of obtaining strain results from the most realistic movement possible. However, as with any computational model, assumptions were made regarding the parameters used in the model. Most of these parameters are dynamic and interconnected. Understanding the effect each assumption has on the model is integral to understanding the model's usefulness. The model's muscle did not include a physiological optimization parameter.

DELIMITATIONS

The subject was recruited from Ball State University. Only one subject was used to develop the model. An active subject was recruited to reduce the potential for injury resulting from a sedentary lifestyle.

SUMMARY

Landing from a jump is a common movement in sport and military situations. High impact forces must be dissipated throughout the body to perform such maneuvers.

While much of the impact is absorbed through soft tissues (muscle and connective tissue) some residual force will be absorbed by bone. As this force acts on the bone, deformation occurs and this deformation can cause microdamage. Bone tissue will repair these small fractures at the cellular level. However, if the repair process cannot keep up with the buildup of microdamage, stress fracture can result. Very little is understood about the biomechanical causes of stress fractures and more research is needed. Previous methods of studying stress fracture included invasive mechanisms [10-16]. Improvements in computational simulation have allowed researchers to look at bone strain using less invasive methods [2]. Information gained from this study will help the research community understand how landing forces influence tibial strain.

CHAPTER 2

REVIEW OF LITERATURE

INTRODUCTION

Large impact forces are transferred through the body during landing. The body uses its muscles and joints to dissipate most of these forces [3]. However, bone will absorb the residual force. The absorption of residual force, while small, can cause microdamage [5]. These small fractures can accumulate and result in larger stress fractures [7].

Bone strain is difficult to study because the biological nature of the material [17]. Improvements in the research methods used to study bone strain allow the researcher to simulate the forces a bone experiences. Simulation can be a tedious process but is significantly less invasive than *in vivo* methods. Studies employing the *in vivo* methods tend to have fewer volunteers willing to submit to the instrumentation procedure. The validation of modeling techniques will allow future research to examine larger cohorts. The result of the research will provide a better understanding of the effect drop landing has on bone strain.

Incidence of Stress Fracture in the Tibia

Breithaupt, a German military surgeon, first described "Fussgeschwulst" or stress fractures in 1855[18]. During World War II large numbers of military stress fractures appeared and have led to continued research in military stress fracture [19]. Stress fractures have continued to be a concern in the military. Armstrong et al. reported that 3% of male and 10% of female Naval Academy recruits experience stress fractures during their first summer of training[20].

It has been suggested that the low level of physical fitness and physical activity prior to entry into the military may be a factor in the development of stress fractures[21]. The rapid change in training regimen does not allow the body to adapt to new stresses. The rigorous training combined with environmental factors including poor footwear, hard training surfaces, and heavy payloads create conditions conducive to stress fractures[9]. Fewer than 30% of Marine recruits were in excellent physical condition according to self reported evaluations at the time of entry[21]. As a result, reports have shown stress

fracture rates ranging from 2% to 12% in U.S. military recruits[20]. Stress fracture is not a problem exclusive to the United States military. Milgrom and his associates have done extensive research in tibial stress fractures in various populations. In one of their studies, they found the Israeli Army to have an incidence of stress fractures near 20% [15].

Military personnel are not the only individuals who suffer from stress fractures. Stress fractures are among the more common injuries resulting from physical exercise[9]. Nearly 10% of all sports related injuries are stress fractures[22]. Brukner summarized literature focusing on stress fractures in sport, primarily in collegiate and elite athletic populations [7]. Two studies assessed athletes in different sports and presented their annual results [23, 24]. Track has the highest incidence but several other sports indicate stress fractures as an injury. Many of the sports where stress fracture is a concern involve jumping and landing. Studies focusing on gymnastics [23, 25], lacrosse [23, 24], figure skating [26] and ballet [27-29] all reported a high incidence of stress fracture. Studies examining stress fracture incidence in basketball ranged from 2.9% to 6.8% [23, 24, 30]. It is important to note that the timeline of these studies varied. The length of the study would have an effect on the total number of fractures reported but not necessarily the rates.

The tibia is one of the most common sites where stress fractures occur. McBryde found that roughly 20% of the stress fractures that occurred in athletes and military personnel are in the tibia[19]. Tibial stress fracture is a common in multiple sports. In a study of 180 stress fractures, Brukner et al. found 36of them in the tibia. Brukner found the tibia to be the most common fracture site in distance runners and Australian footballers [31].

A number of studies have listed the tibia as a primary site of stress fracture in military recruits. In a study including 295 military recruits during basic training, Milgrom et al. found 184 total stress fractures in 91 Israeli soldiers[32]. Milgrom reported 51.2% of the stress fractures were found in the tibia. Other researchers have evaluated the incidence of stress fracture in Naval Recruits. Armstong et al. evaluated 1224 Midshipmen from the U.S. Naval Academy in 2000 [20]. The study found 58 stress fractures (3.3% incidence). Forty three (74%) of the stress fractures in this study were in the tibia. Considerable time is lost when military recruits suffer these injuries.

Etiology of Stress Fractures particularly in the Tibia

Individuals participating in regular physical activity, particularly repetitive movements including running or jumping, are at risk for a myriad of overuse injuries such as Tibial Stress Fracture (TSF) [5, 33]. TSF can result in a loss in training time and money. Stress fractures generally occur when the rate of bone breakdown is greater than the rate of bone formation [7]. Microdamage accumulates and can result in stress fracture.

During physical activity, bone tissue experiences deformation. Deformation is the relative change in shape of an object. Deformation is measured by dividing the change in length of an object by its original length. Strain is the measurement of deformation which is represented in units of strain or microstrain (10^{-6}). Repetitive forces acting on the bone during normal human movement produce strains well below the bone's yield strength [34]. The tibia will normally fracture at 25,000 microstrain or 2.5% deformation [8]. Frost suggests that the safe range is much less concerning irreparable microdamage

[34]. Bone deformation greater than 3000 microstrain can result in diminished remodeling ability [35]. Walking typically creates tibial strains in the range of 250 and 600 microstrain in the tibia [11, 12, 36, 37]. Previous studies involving jumping or landing activities have reported tibial strains between 800 and 2200 microstrain [10, 36]. Unlike other types of fracture, stress fractures are the result of a accumulative process rather than a single application of force to bone [9].

Repetitive forces, such as those experienced during physical activity, can cause bone mass increases [7]. Li et al. examined tibial fracture development resulting from controlled jumping and running in rabbit and concluded that bone necrosis is the initial stimulus for bone resorption [6]. The rabbit tibia contained microscopic fractures or microfractures. Two days after the microfractures were discovered, new bone formation began to occur. This suggests that bone adapts to changes in stress through a process called bone remodeling.

Stress fractures occur when the osteoclastic resorption that normally promotes bone health exceeds the rate of osteoblastic activity. Bone remodeling is the continuous breakdown and repair of cavities in the bone[7]. The purpose of remodeling is to prevent the buildup of microdamage or small fractures [38]. Specialized cells exist in bone tissue: osteoclasts and osteblasts. Osteoclasts resorp or break down old bone while osteoblasts routinely create new bone through the process of remodeling. Repetitive loads lead to increased osteoclastic resorption [39]. Osteoclastic resorption leaves temporary cavities in the bone until the osteoblasts can repair the directed area. If the remodeling process is slower than the resorption, the result is a temporary loss in bone strength [9]. Stress fractures occur when the bone is in this weakened state. The

accumulated microdamage leads to fracture. The accumulation of microscopic fractures is impractical to track making it difficult to predict and ultimately prevent TSF. Instead, focus must be placed on studying the deformation that initiates the remodeling process and determining the strain that bone can safely adapt to.

Common Stress Fracture Sites

Two sites have been identified as predominant sites for TSF: the posteromedial part of the distal tibia and the anterior middiaphysis[36]. Milgrom et al. screened 295 military recruits for stress fractures. Out of the subjects with TSF, 80% were found in the midshaft region[32]. Athletes participating in basketball, workout, tennis, soccer, badminton, sprinting, or mid-distance running showed a tendency towards fracture in the anterior middiaphysis[40]. Stress fractures have been known to occur in this area during participation in sports involving landing. Fractures in the posteromedial part of the distal tibia tended to manifest themselves during long-distance running. Ekenman et al. suggested that these sites may be determined by the musculature involved in a particular movement [36]. This suggests that the area examined during invasive and non-invasive studies should depend on the movement analyzed.

Ekenman et al. investigated the difference in strain values at two sites (posteromedial part of the distal tibia and the anterior middiaphysis of the tibia) when performing various movements. Instrumented bone staples were fixed to a female's tibia in each of the sites identified as being the most common for TSF to occur. The specific sites were 1 cm medial (AM) and 2 cm posteromedial (PD) to the anterior margin of the right tibia. Ekenman et al. found the AM site to have greater tensile (lengthening) strain

while the PD gauges recorded greater strain in compression (shortening). This finding indicates an important consideration of gauge placement must be made when interpreting results of a study because the gauge only records surface strain at the point of attachment.

For the sake of consistency and comparability between studies, the anterior middiaphysis site has been chosen for strain gauge placement most frequently. Lanyon et al. and Burr et al. both used this placement in their early studies on tibial strain [11, 12]. By using the same stain gauge placement site, various studies have been able to conclude whether their findings were consistent or not. The Milgrom et al. *in vivo* studies were very specific about their placement for this reason. An alignment device was used by Milgrom et al. to determine the medial aspect of the tibia where the staple was placed.

Landing Activities and Stress Fractures

Forces acting on the body during drop landing are related to the height of the drop. The kinetic energy of a landing is the result of the potential energy of a body being set in motion. The tissues in the body serve to dissipate the kinetic energy. The body's ability to dissipate the kinetic energy will affect the stresses experienced by the various tissues of the body [1]. Skeletal muscle is responsible for much of this dissipation [41]. In situations where the musculoskeletal system cannot adequately absorb shock, other tissues must dissipate the remaining energy.

Increasing a person's fall height will increase their potential energy. Increased potential energy results in the increased kinetic energy of the person during their fall. Greater kinetic energy leads to greater impulse upon landing which must be dissipated by the musculoskeletal system. Previous research has shown that as the kinetic energy of

the fall increases by elevating the subject the ground reaction force correspondingly increases. Yeow et al. had recreationally active males land from heights of 0.3 and 0.6m. The subjects experienced significantly greater peak vertical ground reaction forces at the 0.6m height when compared to the 0.3m height [1]. Seegmiller & McCaw compared drop landings performed by gymnasts and recreational athletes [42] who experienced increased ground reaction forces as drop height increased. Increased ground reaction forces acting on the body need to be dissipated mechanically or other structures, particularly bone, may be injured.

As ground reaction forces increase with height, there are two possible results: either the tibial strains increase as a result of larger forces acting on it or tibial strain does not increase because the mechanical absorption accommodates the increase in height. Milgrom et al. did not find significant differences in tibial strain during drop landings of different heights [10]. Milgrom et al. suggested that the subjects adapted their landing strategy for the increased height and showed that there was no relation between potential energy and compressive strain in the tibia. The lack of relationship between potential energy and tibal strain suggests that the subjects preferred a strategy that dissipated the increased ground reaction forces. Milgrom et al. suggests that this might be done using muscular shock absorption. Increased muscular forces would result in greater forces acting on the bone at muscle attachment points.

Muscular Strength and Stress Fracture

Skeletal muscle may play a role in both the prevention and development of stress fractures[7]. Muscles serve to dissipate impact forces experienced during movement as a

method of preventing dangerous loads acting directly on the bone[2]. However, the muscular activity from impact absorption applies large forces to the bone at small muscular attachments. While the intent of this absorption mechanism is to protect the bone it may actually cause harm.

Stanitski et al. evaluated 17 patients suffering from stress fractures in the tibia, fibula, and femur[5]. The researchers suggested that the high concentration of force at the muscle attachments during repetitive movements causes large strains to occur at the attachment points. In two of these cases, Stanitski et al. believed the stress fractures were a result of large posterior muscle groups causing increased tensile strain in anterior portion of the tibia during plantarflexion. Repetitive muscle actions cause microdamage at the place of attachment that lead to stress fractures.

Impact loading is not a requirement for stress fracture development. The occurrence of stress fractures in non-weight bearing bones suggests that large strain development at the muscle attachment sites may be a more significant factor in stress fracture development. Stress fractures in the upper extremity during throwing or swimming support the theory that cyclical loading due to muscle activity may result in microdamage build-up.

Scott and Winter [4] used a biomechanical model to assess the forces in three subject's tibiae during running. Previous research had shown that most injuries occurred in the distal third of the tibia. This study looked at forces acting on the bone in this region. They described the three types of loads working in the tibia. Axial forces act parallel to the longitudinal axis of the tibia. Shear forces act perpendicular to the longitudinal axis. The third type of force affecting the tibia is a bending moment. Scott

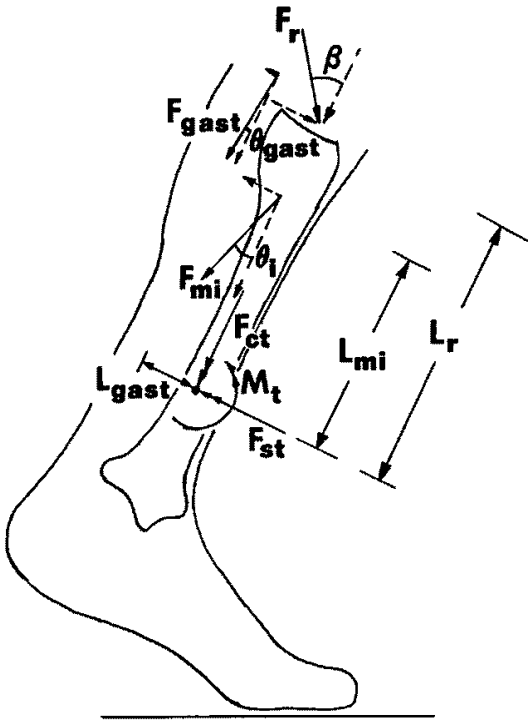

Figure 1: Scott, S.H. and D.A. Winter, *Internal forces of chronic running injury sites.* Med Sci Sports Exerc, 1990. **22**(3): p. 357-69.

and Winter defined the bending moment as the product of the shear force and the distance component. The distance component is the longitudinal distance between the point of application to the distal third of the tibia. The numerous muscle forces acting on the tibia can be summed into one free moment and one force using a couple [43]. Figure 1 from Scott and Winter [4] illustrates the forces and lengths that create the resultant moment. Milgrom et al. believed that bending forces may be the most important type of force when considering stress fracture [15]. Scott and Winter believed that while ground reaction forces cause large bending moments the plantarflexor muscles work to negate them. They found joint-reaction forces creating bending moments between -178 and -285 N·m. The muscle forces created bending moments between 110 and 180 N·m. By adding these two values the result is a total bending moment which is about half of the reaction bending moment (between -85 and -117 N·m). The authors concluded that the plantarflexors create a protective, anti-bending, moment in the lower leg. This conclusion further supports the idea that muscular forces create a complex distribution of forces across the tibia which may affect the creation of TSF.

It seems reasonable to assume that peak strain would occur at peak ground reaction forces, however, this idea ignores the effect that muscular forces have on the tibia. The peak load would depend on the combined effects of ground reaction force and active muscle forces. Lanyon et al. found peak strain at toe-off rather than at foot contact [12]. To further support the influence of muscle forces on strain, the same study found increased strains during running. Forces acting on the bone at toe-off are primarily due to muscle action as the impact phase has past. The tibial strain at toe off in running was greater than in walking.

Improvements in Methods of Studying Bone Strain

There is little research examining the tibial strains in humans during physical activity. A number of studies have used *in-vivo* human tibia strain measurement to collect their data [2, 8, 10-14, 16, 37, 44-49]. Lanyon et al. performed one of the early studies by attaching a rosette-shaped strain gauge to an active male's tibia [12]. The male subject performed a walking and running trial while strain measurements were recorded. They recorded maximum and minimum principal strains of 395 and -434 microstrain respectively while walking barefoot on a treadmill. Maximum and minimum strain values were 311 and -368 microstrain when the subject wore shoes. The effect that shoes have on tibial strain values is one of the primary findings of the study. More importantly, Lanyon et al. demonstrated that it is reasonable to use rosette strain gauges (or instrumented bone staples) to measure deformation in human bone. Ekenman et al. supported this conclusion, finding good intra-test reliability between strain measurements in pig and sheep bone [50].

Burr et al. used a similar instrument to look at strains while two subjects performed military field exercises: unloaded walking, loaded walking, running, and zigzag running [11]. Burr at al. reported maximum and minimum strains of 437 and -544 microstrain respectively during level walking with boots. The strain data in this study was much higher than previously reported by Lanyon et al.

The use of instrumented bone staples posed certain dilemmas in regards to study sample size. Low subject numbers due to the invasive nature of the protocol limited the studies using the staples. The studies conducted by Milgrom et al. had 4.2 subjects on average. Further, many of the subjects were members of the research team. The relatively small pool and sample size brings into question whether their results are representative of larger populations. Another issue that limits these studies is that measurements using the staples are limited to small regions of superficial bones[12]. Less invasive methods for assessing tibial strain are needed.

One method that has become more popular for examining bone properties is finite element analysis (FEA). FEA is a software tool that has been used in many engineering applications to solve complex numerical problems. Using FEA, the researcher can create a model called a finite element mesh (FEM). The researcher can apply simulated loads to the FEM and evaluate the resulting deformation. FEA may be a solution to the hindrance caused by the *in vivo* studies because it is non-invasive and can be repeated for various loading conditions [51].

Potential Drawbacks to FEA

In FEA analyses, bodies are broken down into a finite number of smaller pieces called elements. Elements interact with each other at points called nodes. Each node has individual degrees of freedom which allows it to move in response to a load. A tibia is made up of thousands of nodes whose movement is calculated during finite element analysis. This solution can become extremely computationally expensive meaning that the models require more resources (random access memory) to solve. The cost of such computers (and software) can be a limitation to using this tool. As a result, computation is often simplified by using rigid (non-deforming) bodies, by focusing on a small portion or phase of a movement, or evaluating static situations only [2].

Methods of model simplification can save on the computational cost of the analysis. Using the assumption that bone behaves linearly for the range of strain [52], this simplification can be employed. The Crag-Bampton modal analysis method is a model simplification method that evaluates an object's response to different vibrational frequencies [53]. Modal coordinates are associated with the deformation modes at different frequencies. This procedure substantially reduces the number of degrees of freedom, which reduces the computation time without significantly affecting the accuracy of the analysis[54]. The Craig-Bampton analysis can be run within the MD Adams platform (MSC Software Corporation, Santa Anna, CA) upon which LifeMOD is built.

PID Controllers and Musculoskeletal Simulation

To understand the musculoskeletal modeling process, a general knowledge of Proportional-Integral-Derivative controllers is essential. PID controllers were originally

used in autopilot mechanisms in ships during the early 20th century[55]. This method of control is popular because of its simplicity and proven success. PID controllers are three-term algorithms, which use a target point to control a system. The error between the estimate and the target is used to make corrections to the estimate. The calculation used in the PID controller is the weighted sum of the three terms: proportional, integral, and derivative. A graphical representation of the PID control can be found in Figure 2 from Johnson [56]. Each term has a gain value associated with it, *k*. The proportional term makes a correction that is proportional to the size of the error. This part of the algorithm is represented by $\boldsymbol{u_c(t) = k_p e(t)}$, where $\boldsymbol{e(t)}$ is the system error sent to the controller and $\boldsymbol{u_c(t)}$ is the output control signal. The integral term is represented by the equation, $\boldsymbol{u_c(t) = k_I \int^t e(\tau) d\tau}$. This part of the calculation accounts for steady offsets from the signal. The advantage that the integral term offers is to eliminate this offset (which the proportional term cannot) without increasing the gain significantly. The final term, derivative or differential, is given by the equation $\boldsymbol{u_c(t) = k_D \frac{d\, e(t)}{dt}}$. The derivative term uses the rate of change of the error signal to help the prediction and improve the control response. Much of the continued research in the area of PID control has sought to improve the accuracy and ease of tuning the controller. This means tweaking the gains for each of the parameters.

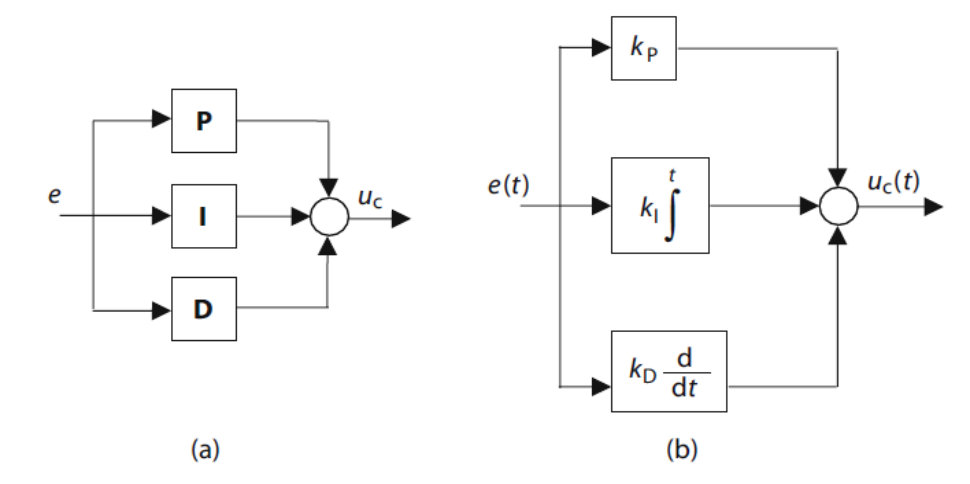

Figure 2: Johnson, M.A., M.H. Moradi, and J. Crowe, *PID control : new identification and design methods.* 2005, New York: Springer. xxvii, 543 p.

When applied to the muscle elements in the model, PID controls use the target length/time curve as their desired signal. The control in LifeMOD follows the equation:

$$F = k_p P_{error} + k_I \int^t P_{error} d\tau + k_D \frac{d\, P_{error}}{dt}$$

Where:

$$P_{error} = \frac{target\ value - current\ value}{range\ of\ motion}$$

Working backwards, LifeMOD solves for P_{error} using the target muscle length/time curve and current signal. By calculating the sum of the three weighted terms, the muscle force needed to create a desired muscle length can be determined. The maximum muscle force is limited by the physiological constraints of each muscle (determined by LifeMOD). This force causes a change in muscle length, which moves the segments in the model. The controller input is the comparison between the target length and current length. The parameters were tuned specifically for this process. Once the gain values are set for each controller for each muscle, the motion can be simulated. The PID controller makes

changes to the force which are then exhibited as changes in muscle length. The forward dynamic simulation uses the PID controllers in each muscle to closely mimic the length/time curve from the inverse kinematic simulation.

Adding Muscle to the Model

It is now possible to use a flexible body in combination with Multibody Dynamic Simulation (MBD). In MBD, changes can be made to systems involving multiple parts in order to simulate the changes that would result. MBD software designed specifically for biomechanical simulation use the musculoskeletal system as a model. By combining these two tools, simulations which include bone and muscle interactions can calculate the deformation of a bone.

The musculoskeletal models use kinetic and kinematic data from motion capture to determine the loading of the joints and skeletal structures. Using the captured data along with a musculoskeletal model, the FEA can provide a more realistic simulation of stresses and strains. Al Nazer et al. first applied this method using a generic lower body skeletal model generated from the Generator of Body Data (GeBOD) database in LifeMOD (LifeModeler, San Clemente, CA) [2]. The lower body segments were all treated as rigid bodies except for the right tibia which was used for the flexible body portion of the analysis. Al Nazer et al. evaluated one subject performing barefoot walking trials. Data from the motion capture

Muscle	γ-value
Gluteus Medius	0.75
Biceps femoris	0.33
Rectus femoris	0.22
Vastus Lateralis	0.65
Soleus	0.94
Tibialis	0.39

Table 1: Al Nazer, R., et al., *Flexible multibody simulation approach in the analysis of tibial strain during walking.* Journal Of Biomechanics, 2008. **41**(5): p. 1036-1043.

was used to control the model in an inverse dynamic simulation. The inverse dynamic simulation served to record the muscle length/time patterns. In the forward dynamics simulation, the PID controlled muscles attempted to replicate the patterns recorded during the inverse kinematic simulation. Maximum and minimum principal strain values were calculated. A cross-correlation coefficient (γ) was used to compare ground reaction forces and muscular activation patterns of the model and experiment. A comparison of the ground reaction forces yielded a γ value of 0.97. Table 1 lists the muscular forces which yielded varying γ values.

Al Nazer et al. compared the results from the modeling method to four previous *in vivo* studies. Two of the four studies were explained earlier, Lanyon et al. and Burr et al. The remaining studies, those of Milgrom et al, involved four and six subjects and reported strain data comparable to the Al Nazer study. Table 2 lists these comparisons. The principal strains in the Al Nazer et al. study fell within 23% and 20 % of the Milgrom et al. studies. Al Nazer et al. felt that this was a reasonable agreement between the simulation and the *in vivo* studies previously conducted. Al Nazer et al. had several limitations that future studies can focus on in an effort to more accurately simulate tibial strains and strain rates.

Drop landing has shown to produce lower strain rates than running[10] which may be a result of muscular shock absorption. However, as noted earlier, the low strain rates tend to cause the accumulation of microdamage and ultimately create fractures. The proposed study will compare tibial strain rates produced while performing drop landings from three different heights.

Summary

Landings are often performed in military and athletic movements. Drop landings produce impact forces which must be dissipated. The human body dissipates these forces in a few different ways. Much of the impact force is dissipated through the landing strategy. Not all of the force from landing is absorbed by the soft tissues. The remaining force is absorbed by bone. This force initiates the remodeling process. If bone remodeling cannot keep up, the microfractures may ultimately result in a stress fracture. Research on stress fractures has been limited mainly due to the invasive methods used. Improvements in study design have sought to create valid methods of simulation using FEA and MBD to circumvent the use of *in vivo* tools. These methods have the potential to make it easier to include larger samples in studies.

CHAPTER 3

METHODS

INTRODUCTION

The purpose of this study was to develop a computational model and measure strain and strain rate in the tibia while landing from various heights. The subject

had his tibiae imaged using a CT scan at Ball Memorial Hospital prior to the collection. Three different heights were used to examine the differences in tibial strain that exist when landing. The subject performed at least three landings from each of the three heights. Kinetic and kinematic data were recorded during the collection. The simulation process used the collected data to run a simulation of the tibial deformation during the performance of the landing. This study was carried out in the Ball State University Biomechanics Laboratory in compliance with the Ball State University Institutional Review Board (IRB).

EXPERIMENTAL PROCEDURE

Subject Description

One healthy male subject participated in this study. The subject was 22 years old at the time of the study. The subject had a mass of 78.6 kg and a height of 1.85 m. It is also important to note that the subject's right leg, the one used to kick a ball, was determined to be the dominant leg.

Experimental Overview

Prior to data collection, the subject had a CT scan on both of his tibiae in conjunction with another ongoing study in the Ball State University Biomechanics Laboratory. The subject reported to the Ball State University Biomechanics Laboratory on the day of his scheduled data collection. The subject reviewed the consent form with the principal investigator. Once all of his questions were answered, the subject signed

two copies (one for lab records and one to keep) in accordance with the Ball State University Institutional Review Board.

After signing the consent form, the subject was prepared for the data collection. The subject was given attire that aided in the data collection. The shirt and shorts had Velcro patches to attach specific markers. The subject's anthropometric measurements were taken. Anthropometric measures included height, mass, leg length, and widths of the ASIS, knees, and ankles. The surface EMG electrodes were attached to the vastus medialis, vastus lateralis, medial hamsring, medial gastrocnemius, tibialis anterior, and soleus muscles using custom stickers. The research team performed manual resistance tests to confirm the placement of each electrode. Once the electrode placement was confirmed, reflective markers were attached to the subject according to a cluster-based marker set. Six clusters were attached to the subject: one on each ASIS, thigh and shank. The ASIS clusters had 2 markers each while the leg clusters had 4 markers each. Markers were attached to boney landmarks on the subject's lower body joints. At this point the subject was ready to begin the data collection.

The subject was instructed on how to step off the box but not in landing technique. Since subjects tend to perform similar landings from one trial to the next when allowed to self-select a strategy[10], it was necessary that the subject choose a preferred landing strategy. To achieve this, the research team was careful to give specific instructions regarding the take off only. The subject was given a chance to practice 5 landings before data collection began. The randomly selected order of landing heights for this subject was 26, 39, and 52 cm.

The three drop landing heights followed the protocol used in a previous study [10] allowing the comparison to *in vivo* data. The subject performed at least three landings from each of the three heights. Trials were checked to confirm marker visibility. Any trials with missing markers were repeated. Nine acceptable trials were collected.

Data Collection

A 16 channel Bagnoli Desktop EMG system (Delsys Inc. Boston, MA) was used to record surface EMG data at 2400 Hz. A 14 camera (VICON F-series, Vicon, Oxford, UK) motion capture system controlled by VICON Workstation software collected motion data. Kinematic data were collected at 120 Hz. Kinetic data were collected at 2400 Hz using two AMTI multi-axis force platforms (Advanced Mechanical Technology, INC. Watertown, MA).

In preparation for the EMG electrodes, the placement sites were cleared of hair and dead skin using a razor, sandpaper, and isopropyl alcohol. EMG electrodes captured the activity of the vastus medialis, vastus lateralis, medial hamstring, medial gastrocnemius, tibialis anterior, and the soleus in both legs. Electrode placement sites were selected according to Cram's Introduction to Surface Electromyography [57]. The subject performed toe and heel raises to verify proper electrode placement on the medial gastrocnemius, tibialis anterior, and the soleus. A member of the research team held the subject's ankle and added resistance while the subject performed knee flexion and extension movements. This was used to verify electrode placement on the vastus medialis, vastus lateralis, and the medial hamstring. An experienced member of the

research team reviewed the graphs and confirmed that the EMG electrodes were in the proper position to receive quality signals.

Reflective markers were attached to the skin on bony landmarks using double-sided tape. This study used a cluster-based marker set utilizing calculated functional joint centers[58]. Clusters are a group of markers attached to a plate which is then attached to the subject's body using either double-sided tape or by wrapping Powerflex® (Andover Healthcare, Salisbury, MA) around the limb and cluster**.** Three markers are necessary to calculate the translational and rotational movement of the segment. An additional marker was attached to the cluster to prevent the potential loss of data resulting when one marker is covered or missing. One 4-marker cluster (Figure 2) was attached to each thigh and shank using Powerflex® and athletic tape. 2-marker clusters were taped to the anterior superior iliac spine (ASIS). The Plug-in-Gait (Vicon Oxford, UK) bony landmarks used were the posterior superior iliac spine (PSIS), lateral knee femoral epicondyle, lateral malleolus, calcaneous, toe, and first metatarsal joint. In addition to the Plug-in-Gait (PiG) landmarks, markers were attached to the medial knee femoral epicondyle, medial malleolus, and near the distal head of the fifth metatarsal. A pelvic crest marker was attached to a Velcro patch on the shorts. Three markers were attached to the Velcro on the subject's shirt. These markers were used to track the upper body movement but were not used in this study.

Figure 3 Left- Reflective Marker. Right- Cluster Marker.

Once the subject was prepared, the motion capture collection began with a static calibration. The subject stood in a T-pose with his arms out to the side holding a marker wand. The research team collected a short clip of this position to calibrate the labeling feature in Vicon Workstation. The PSIS and medial joint markers were only necessary for the static trial and were removed. Virtual landmarks were created using a digitizing wand with markers of known positions. This method can be used when there are landmarks needed for the motion capture but cannot be marked in the usual fashion. In the case of this study, virtual landmarks aided in guiding the tibia into position prior to forward dynamic simulation using the flexible tibia. A member of the research team pointed the wand at three landmarks near the proximal head of the tibia. Coordinates for the tibial tuberosity, medial and lateral ridges of the tibia were stored in the C3D.

The final step in the calibration trials were to collect the range of motion (ROM). ROM trials were performed for both knees and both hips. While performing the ROM trials the subject was asked to stand sill and move a single joint in a specific pattern but not in his full range of motion. To perform the hip ROM, the subject was instructed to move his foot in a five pointed star pattern followed by one circumduction. To perform the knee range of motion the subject was instructed to flex and extend his knee five times. These trials allowed the research team to create functional joint centers. The use of functional joint centers is particularly important to the accuracy of the motion capture analysis as it reduces the impact of marker placement error on joint location[58]. This method of estimating the functional joint center was first described in the literature by Schwartz and Rozumalski[58]. Schwartz and Rozumalski based their design on the assumption that two adjacent segments of the body share one common point, the joint

center[59]. Through these movements, a determination of the subject's joint center could be made.

The movement trials were conducted after the preparation was complete. The subject was given minimal instruction on how to step off of the height. The leg the subject used to kick a ball was designated as his dominant leg. The subject stood on the box suspending the dominant foot directly in front of the box. The subject was positioned on the elevation so that each foot would land on a separate force plate. To begin the movement, the subject shifted his weight forward and stepped off from the height. The subject landed on both feet simultaneously. Each of the subject's feet landed on a separate force plate. The three heights were created using a combination of boards, aerobics steps and lifts. The specific combinations were prepared before the data collection.

The subject performed three landings from each height: 26, 39, and 52 cm. The heights were taken from a previous Milgrom et al. method[10]. Any trials with missing markers were repeated. Once three acceptable trials had been collected from the first height, the research team set up the next height. After all three heights had been collected the motion capture portion of the study was complete.

Overview of Modeling Procedure

The motion capture data was processed using Visual 3D (C-Motion, Germantown, MD). Filtered force and marker data were exported from Visual 3D and converted to a LifeMOD file format (*.slf file) using custom MATLAB (MathWorks Natick, MA) code. The static model was created and calibrated in LifeMOD (BRG, San Clemente, CA)

using the .slf files. A more detailed description of the .slf file can be found in the Matlab Appendix (Appendix C). LifeMOD allowed the research team to simulate muscle forces during the movement trials. The simulated muscle forces were used with the kinematic and kinetic data to calculate the deformation of the flexible tibia created in MD Marc (MSC Software Corporation, Santa Anna, CA) using the Adams Durability (MSC Software Corporation, Santa Anna, CA) plug-in in LifeMOD.

MODEL DESIGN

Flexible Tibia Creation

The flexible tibia FEM was created in Mimics 13.1 (Materialise, Ann Arbor, MI) and MD Marc before the any simulation was run in LifeMOD. The tibia scans were imported into Mimics 13.1. CT scans were chosen over other imaging processes because of its ability to depict bone. 512 pixel x 512 pixel slices of the tibia were scanned using a slice thickness of 0.625 mm. The scan was digitized in Mimics through a process called segmenting where the shape of the bone is outlined on each slice. Mimics stacked each outline to create a 3-dimensional, geometric representation of the tibia. It was found that using custom settings to create the object worked best. The object was smoothed using a 1^{st} order Laplacian method with 3 iterations and a smooth factor of 0.9 in the Mimics remesher. The default settings were then used in the Reduce and Auto-Remesh functions. The number of elements were reduced to improve processing speed in MD Marc. The remeshed object was then exported as a surface mesh (DXF).

The DXF was opened in MD Marc. The volume mesh was created using 3mm x 3mm x 3mm hexagonal elements. Bone is transversely isotropic within the ranges of strain we are evaluating [49, 52] meaning that its material properties are the same in every direction in the transverse plane. Previously reported isotropic material properties were assigned to the elements [60]. The stiffness of the bone was set using a Young's Modulus of 17 GPa [2]. The Poisson's Ratio was set at 0.3[2]. The Mass Density was set at $1.9x10^{-6}$.

The flexible tibia is brought into LifeMOD and aligned to the model in the static trial. The researcher manually aligned the tibia using the knee and ankle joint axis as a reference. Once aligned the attachment sites are exported. A custom Python (Python Software Foundation, Wolfeboro Falls, NH) script ran in MD Marc used the attachment points from LifeMOD to create the rigid body elements (RBE's) representing the ankle and knee joints as well as the muscle attachments. An RBE type 2 was used to rigidly attach the nodes representing joints and muscles (reference nodes) to nodes on the flexible tibia (tied nodes). RBE2's create a rigid link between the reference node and the tied nodes. Once the RBE2's were created, a modal analysis was run in Marc/Mentat using the Craig-Bampton method. Mentat creates a modal neutral file (MNF) once this analysis is complete. The MNF contains information regarding the tibial geometry, nodal mass, and stiffness. Most importantly, the MNF contains the modal responses which allow us to examine the nodal movement resulting from the simulated drop landing.

Musculoskeletal Model Creation

A lower body model was created in LifeMOD using the static trial. The model consisted of seven segments: a pelvis, two thighs, two shanks, and two feet. LifeMOD used the subject's measurements (height, mass, sex, and age) to create the segments. A file containing the location of the subject's joints from the static trial was applied to the model. The segments were scaled to the joint locations and the markers were added to the subject. A 17-muscle set was added to the model's right leg. Muscles were only used to control movement in the right leg. The standard PiG markers from the static trial were used to set the model's initial posture. Since the marker set included markers beyond the standard PiG set, additional markers were added to the model using augmented sets. This was considered the calibrated model.

Once the muscles were added, the inverse kinematic simulation was run using the prepared motion capture data. During the inverse kinematic run, the movement of the model was controlled by the motion capture data. A series of files containing the motion of the markers were imported and applied to the calibrated model. As the simulation was carried out, length/time curves of each muscle were passively recorded [61]. The length time curves served as the target for the PID controllers. The parameters were selected for the model. Once the gain values are set for each controller for the muscles, the motion can be simulated. The forward dynamic simulation uses the PID controllers in each muscle to closely mimic the length/time curve from the inverse kinematic simulation.

The forward dynamic simulation used the muscles to control the movement. All of the markers were removed except the right thigh markers, which were still needed to

control the motion of the hip. The left leg joints were controlled using servos. Without the motion agents, the motion of the model was controlled by the muscles. The length/time curves of the muscles served as a target for the PID controller.

The final step in the simulation process was the flexible analysis. The flexible tibia with the rigid body elements (the MNF) was included in the musculoskeletal model in LifeMOD. The MNF is imported and the simulation is run with the same settings as the forward dynamics simulation. Using the Adams/Durability plug-in for LifeMOD, the strain values were calculated for six nodes. The six nodes were hand selected by a member of the research team to represent the area where the staple was placed during *in vivo* studies [36]. The same six nodes were used in each trial. This simplification allowed for comparison to *in vivo* studies. The Durability plug-in recorded maximum principal, minimum principal and shear strain data. Principal strain is the strain, in a single element, along the three principal axis [62]. Any strain can be broken down and represented as along the principal axis. Shear strain acts perpendicularly to the maximum and minimum principle (tensile and compressive) strain.

DATA MANAGEMENT

Data Processing

Motion capture data was reconstructed in Vicon Workstation using values selected specifically for drop landing. Previous research on landing motion was used to

design the filtering pipeline in Visual 3D [63]. Motion data was filtered at 10 Hz and analogue data at 60 Hz. The filtered data was used for the simulation.

A Fast Fourier Transform (FFT) was performed on the nodal strain values using PSIPlot (Poly Software International, Pearl River, NY). The FFT revealed that much of the signal occurred at a frequency less than 5 Hz. However, some portion of the signal appeared around 20 Hz. Previous research suggests that most bone strain occurs at about 3 Hz [64]. Turner et al. examined bone strain in canines while walking and standing. This study found that bone strain existing in the 15-30 Hz range was only 4% of the magnitude of strain values in the 0-2 Hz range. As a result, the data in the current study was filtered using a second order, lowpass, Butterworth filter with a cutoff frequency of 5 Hz. This study was interested in the variation in peak strains. Any true strains occurring greater than 5 Hz is likely to be insignificant as their magnitudes are much less.

Muscle activation was important in comparing the captured movement to the simulated movement. Muscle activation was collected with using the surface EMG electrodes. The modeled muscle forces were used to represent the muscle activation patterns in LifeMOD. The method of comparing muscle activity was previously described by Al Nazer et al [2]. A custom pipeline was created in Visual 3D to process EMG data. EMG signals were rectified, zeroed, and filtered using a lowpass Butterworth filter with a cutoff frequency of 10 Hz. The muscle forces were filtered at 5 HZ in LifeMOD. Both the EMG and the muscle forces were normalized to their maximum value for comparison. Normalized EMG data were compared to the normalized muscle force data from the simulation in accordance with the previous method [2].

The final issue related to data processing was the sampling rates. As earlier noted, analog data was collected at 2400 Hz and kinematic data was collected at 120 Hz. The forward dynamic simulation was modeled at 100 Hz. Data must be resampled in order to compare the collected to the modeled data. Custom Matlab code was written to convert the higher frequency signals to the lower.

Data Analysis

SPSS v16 (SPSS Inc. Chicago, IL) was used for statistical analysis. The accuracy of the computational model was verified by comparing the kinematics from the motion capture and the simulation as well as comparing the simulated leg muscles forces from to the corresponding collected EMG data. Cross-correlation functions were used for the comparisons [2]. Specifically, joint angles (hip, knee, and ankle) of the right leg from the forward dynamic simulation were compared to their correspondences from the motion capture of the 26cm landing condition. Simulated leg muscle forces from LifeMOD were compared to the corresponding leg muscle EMG data during one trial at each of the three landing heights. The cross correlation examines the covariance between two signals [65-67]. This analysis calculates the point-by-point correlation between the two signals while shifting one relative to the other [68, 69]. The shift, or lag, is used to calculate correlation regardless of the time-lag that may be present. Each lag is equal to one time point. The number of lags examined was selected based on the amount delay we expected to see in two signals. Since data were compared at 100 Hz, each lag was 0.01 s. A cross correlation with 15 lags in both directions was used to compare the processed

EMG to the simulated muscle forces. Captured and simulated joint angle data were compared using a cross correlation with 10 lags in both directions.

The second step in data analysis was to compare strain and strain rate values from the different heights. Since this study used only one subject, typical mean comparison methods such as the student's t-test or ANOVA were considered inappropriate. Instead, the effect size (Cohen's d) was calculated [70]. The effect size calculates a standardized difference in means or the magnitude of the difference of a single variable [71]. This tool is useful in assessing differences in data which may be skewed as a result of either a large or small sample size [70]. The effect size indicates more of the practical or clinical importance of data than measure focused solely on significance [71].

CHAPTER 4

RESEARCH ARTICLE

A NOVEL APPROACH TO ESTIMATING TIBIAL BONE STRAIN RESULTING FROM DROP LANDINGS

Original Article

Scott S. Dueball[1], Henry Wang[1], Eric L. Dugan[2], and Lisa Jutte[1]

[1]*School of Physical Education, Sport, and Exercise Science, Ball State University, Muncie, IN 47306, USA*

[2] *Department of Kinesiology, Boise State University, Boise, ID, USA*

Plans to submit to:

Journal of Biomechanics

Keywords: Musculoskeletal modeling, FEA,

ADDRESS FOR CORRESPONDENCE:

Scott S. Dueball

Biomechanics Laboratory
Ball State University
McKinley Avenue, PL 202
Muncie, IN 47306
Phone: (Int+1)(765) 285-5178
Fax: (Int+1)(765) 285-8762
Email: scott.s.dueball@gmail.com

ABSTRACT

During landing, the human body is required to absorb impact forces throughout its tissues. Muscle and connective tissue is able to dissipate much of this force, however, a portion of the impact is delivered to the bones. Forces acting on the human skeleton can cause microscopic fractures which may lead to stress fracture. The present study seeks to calculate changes in the magnitude of strain using noninvasive methods. A musculoskeletal model representing a healthy male subject (22 years, 78.6 kg, 1.85 m) was created. A flexible tibia, created from a computed tomography scan of the subject's right tibia, was included in the model. Motion capture data were collected while the subject performed drop landings from three separate heights (26, 39, and 52 cm) and used to compute simulations in LifeMOD. Surface electromyography and joint angle data were compared to their simulated counterparts using a cross correlation. Maximum magnitudes of principal and maximum shear strain were computed. The model had reasonable agreement between joint angle curves. A large Cohen's d effect size showed that our subject had increased tibial strain and strain rate as the drop height increased. This study demonstrates a valid method of simulating tibial strain during landing movements. Future studies should focus on recruiting a larger sample and applying this method.

INTRODUCTION

The body's ability to dissipate the landing impact will affect the stress and strain experienced by the various tissues of the body [1]. The skeletal system, working mechanically as a series of levers, is responsible for much of this dissipation [2]. In situations where the musculoskeletal system cannot adequately absorb the impact mechanically, bone must dissipate the residual force. Stress fractures result from the deformation caused by this residual force.

Breithaupt first described "Fussgeschwulst" or stress fractures in 1855[3]. During World War II, large numbers of military stress fractures appeared and have led to continued research [4]. Stress fractures have continued to be a concern in the militaries throughout the world [5-8]. The vigorous training combined with environmental factors including poor footwear (boots), hard training surfaces, and heavy equipment create conditions conducive to stress fractures[6]. Rapid changes in training combined hard training surfaces exist in sport and may be resulting in high numbers of stress fracture as well. Nearly 10% of all sports related injuries are stress fractures[9]. Several sports which have reported a high incidence of stress fracture involve drop landings [10-16]. The tibia is a primary concern when examining stress fracture incidence as it has been identified as one of the most common locations of stress fracture in both military and athletic populations [4, 5, 17, 18].

Absorption of residual force can cause microdamage in the bone tissue. These microscopic fractures will accumulate and may result in larger stress fractures. Unlike other fractures, stress fractures are the result of a chronic process rather than a single application of force to bone [6]. Repetitive forces acting on the bone during normal

human movement produce strains well below the yield strength of bone [19]. These repetitive forces cause microdamage. Bone tissue regularly repairs microdamage through remodeling [20, 21]. During remodeling, osteoclasts break down damaged bone and osteoblast form new bone. The break down, called resorption, leave temporary cavities which the osteoblasts must repair. When the osteblastic repair is slower than the osteoclastic resorption the result is a loss in bone strength [6]. The accumulation of unrepaired microdamage leads to fracture. Bone deformation led to microscopic fracture just prior to repair in rabbit tibiae [21]. A better understanding of the strains leading to stress fracture can be gained by examining bone deformation.

One method of examining tibial stress fracture (TSF) risk is by measuring deformation. Researchers have measured tibial deformation *in vivo* using instrumented, strain gauges [22-25]. These studies require instrumentation that is surgically implanted on the subject's bone. *In vivo* studies generally have fewer volunteers due to their invasive nature. The instrumentation examines only surface strain on a small area of bone posing another limitation to this method. Recently, non-invasive protocols involving computer simulation have been used to examine tibial strain [26, 27]. Advances in musculoskeletal modeling have allowed researchers to apply captured human motion to computer models to evaluate tibial strain.

Musculoskeletal models consist of a skeleton controlled by links representing skeletal muscle. The bones of the skeleton are modeled as rigid or non-deforming bodies. Muscle forces are simulated using progressive-integral-derivative (PID) controllers [28]. PID control is a 3-term control method which uses the error in estimation to improve the output accuracy [29]. PID controllers simulate the movement by developing the

necessary force to replicate change in length of the muscles (length/time curve). The control uses the error in each length/time curve to correct the force necessary to reproduce the movement [28]. Changes made to individual muscles affect the entire model. The process creates a solution that allows the muscles to work in unison to move the entire model appropriately.

To examine bone deformation a flexible body representing the bone is added to the musculoskeletal model. Using finite element analyses (FEA), the tibia is broken down into a finite number of small pieces. The tibia mesh is made up of thousands of nodes whose movement is calculated during finite element analysis. The number of degrees of freedom (DoFs) make this solution computationally expensive. The inclusion of skeletal muscles in a dynamic solution seems almost impossible.

Methods of model simplification can reduce the computational cost of the analysis. Al Nazer et al. used modal tendencies rather than movement of individual nodes to examine tibial deformation during gait [26]. Modal analysis evaluates an object's response to different vibrational frequencies. This procedure substantially reduces the number of degrees of freedom without significantly affecting the accuracy of the model [30]. The goal of this study was to develop a computational model utilizing modal analysis to examine tibial strain during landings from different heights.

METHODS

A healthy Caucasian man (22 years, height 185 cm, mass 89 kg, right leg dominant) volunteered for the study. Prior to data collection, the subject had a CT scan of

of his right tibia. The subject reviewed and signed the consent form approved by the University Institutional Review Board before participating in the study.

The subject was barefoot and clad in skin-tight clothing. Reflective markers were attached to the subject's bony landmarks. This study used a cluster-based marker set utilizing calculated functional joint centers [31]. The modified full body Plug-in-Gait (PiG) marker set (Vicon, Oxford, UK) was used with additional markers placed on iliac crests, medial femoral epicondyles, medial malleoli, and the bases of the first and fifth metatarsals. In addition, marker clusters were placed on the thighs and shanks to assist in tracking the leg motion. EMG electrodes were attached to 6 muscles on each leg: the tibialis anterior, soleus, vastus mediali, vastus lateralis, lateral hamstring, and medial gastrocnemius according to Cram's Introduction to Surface Electromyography [32]. Three dimensional coordinates of the reflective markers were captured at 120 Hz using a fourteen camera (VICON F-series, Vicon, Oxford, UK) motion capture system controlled by VICON Workstation software. Ground reaction force data was collected at 2400 Hz using two AMTI multi-axis force platforms (Advanced Mechanical Technology Inc., Watertown, MA). Lower body muscle activity was recorded using a 16-channel Bagnoli Desktop EMG system (Delsys Inc., Boston, MA) at 2400 Hz.

The subject performed the drop landing movement with the non-dominant foot on the box and the dominant foot suspended directly in front of the box. To begin the movement, the subject shifted his weight forward and stepped off from the height. The subject landed with each foot on a separate force plate simultaneously. The subject was instructed to land and remain standing until the research team completed capturing the

trial. The subject performed landings at each height: 26, 39, and 52 cm [25]. Three acceptable trials were collected from each height.

The motion capture data were reconstructed in Workstation and processed using Visual 3D (C-Motion, Germantown, MD). Motion and force data was filtered using a lowpass butterworth filter with cutoff frequencies of 10 and 60 Hz respectively in Visual 3D. Filtered kinetic and kinematic data were exported from Visual 3D and converted to a LifeMOD file format (*.slf file) using MATLAB (MathWorks, Natick, MA).

Finite Element Procedure

The flexible tibia finite element mesh (FEM) was created using Mimics 13.1 (Materialise, Leuven, Belgium) and MD Marc (MSC Software Corporation, Santa Anna, CA) prior to the simulation in LifeMOD. 512 pixel x 512 pixel slices of the tibia were scanned using a slice thickness of 0.625 mm. A surface mesh was created from the tibia scans using Mimics 13.1. CT scan was chosen over other imaging processes because of its ability to depict bone. A volume mesh was created from the surface mesh in MD Marc using 3mm X 3mm X 3mm hexagonal elements. Material properties were assigned assuming that bone is transversely isotropic within the ranges of strain we evaluated [33-35]. A Young's Modulus of 17 GPa [26], Poisson's Ratio of 0.3[26], and Mass Density of 1.9x10-6 were assigned from previously reported values.

Modeling Procedure

A lower body model was created in LifeMOD (BRG, San Clemente, CA) based on the subject's height, mass, age, and sex. The model, shown in Figure 1, consisted of

----------Insert Figure 1 here----------

seven segments: a pelvis, two thighs, two shanks, and two feet. The segments were scaled to the joint locations and the markers were added to the model. All of the segments were assumed to be rigid bodies except for the right tibia finite element mesh, which was assumed to be a flexible body. Material properties were assigned to the finite element mesh using the assumption that the finite element mesh was transversely isotropic. The right side of the model was actuated by 17 muscles, while the left side was controlled using motion-replicating servo controlled joints. Marker data was retained from the right thigh cluster to create more desirable hip motion than the muscles alone could replicate.

After the muscles were added, the segments were scaled to the joint center locations. The standard PiG markers from the static motion capture trial were used to set the model's initial posture. Since our marker set included markers beyond the standard PiG set, the additional markers were added to the model. Length/time curves of the muscles were recorded while motion data controlled the movement of the limbs. The simulation then replicated the movement using the recorded muscle patterns.

The final step in the simulation process was the flexible body analysis using the finite element mesh tibia. Rigid body elements (RBE2), representing the knee and ankle joints, constrained the flexible tibia in the musculoskeletal model. RBE2's also created the muscle attachment sites on the tibia. The Craig-Bampton method was used to calculate the modal responses to different vibration frequencies [36]. The modal analysis returns a file containing the tibia's stiffness and modal tendencies which is imported into LifeMOD to use in the forward dynamic simulation. The strain values were obtained from the location previously described: the medial aspect of the mid-tibial diaphysis [37].

This simplification reduced the computational cost of running the simulation and allowed for continuity with previous research. The Durability plug-in recorded maximum and minimum principal strain data as well as shear strain data for the flexible tibia.

Data Analysis

Collected data was processed prior to performing statistical analysis. EMG data were processed following the method described by Al Nazer et al. [26]. EMG data were rectified, zeroed, and filtered using a lowpass Butterworth filter with a cutoff frequency of 10 Hz using a custom pipeline in Visual 3D. The muscle forces were filtered at 5 Hz in LifeMOD. Both the EMG and the muscle forces were normalized using the maximum value of each curve.

Previous research suggests that most bone strain occurs at about 3 Hz [38]. Further, bone strain within the 15-30 Hz range were only 4% of the magnitude of strain values in the 0-2 Hz range. As a result, the strain data in the current study were filtered using a second order, lowpass, Butterworth filter with a cutoff frequency of 5 Hz. Strain rate was calculated by dividing the change in strain by the time step. Maximum values were selected from each trial and averaged.

To verify the accuracy of the model, simulated joint angles and muscular forces were compared to the measured joint angles and EMG from one trial at each height using a cross correlation coefficient in SPSS v16 (SPSS Inc., Chicago, IL). The analysis calculates the point-by-point correlation between the two signals while shifting one relative to the other [39, 40]. The shift, or lag, is used to calculate correlation with respect to time-lag that may be present. Each lag is equal to one time point. The number of lags examined was selected based on the amount delay that might exist between the two

signals and the source of the signal (marker data or EMG). Since data were compared at 100 Hz, each lag equals 0.01 s. A cross correlation with 15 lags in both directions was used to compare the processed EMG to the simulated muscle forces. Captured and simulated joint angle data were compared using a cross correlation with 10 lags in both directions. The maximum cross correlation coefficients were reported.

A Cohen's d effect size was used to analyze differences in tibial strain magnitudes between the different heights [41]. The effect size calculates a standardized difference in means. This tool is useful in assessing differences in data which may be skewed as a result of either a large or small sample size[42].

RESULTS

Visual inspection of Figures 2-4 demonstrates the similarity between the joint angles in Visual 3D and LifeMOD. Strong cross-correlation-coefficients were found between the Visual 3D and LifeMOD joint angles at lags of 0.01 seconds or less (Table

----------Insert Table 1 here----------

----------Insert Figure 2 here----------

----------Insert Figure 3 here----------

----------Insert Figure 4 here----------

1). Figures 5-7 illustrate the similarity between the collected EMG activity and the muscle forces in LifeMOD. Table 2 lists the cross-correlation between the muscle activation patterns (EMG and forces). Three of the muscles, the medial gastrocnemius, vastus medialis, and vastus lateralis had cross-correlations greater than 0.7 at lags less than 0.15 seconds at all three heights. The peak gastrocnemius coefficient occurred at the

----------Insert Table 2 here----------

----------Insert Figure 5 here----------

----------Insert Figure 6 here----------

----------Insert Figure 7 here----------

longest lag in all three trials: 0.12, 0.15, and 0.11 for the 26cm, 39cm, and 52cm trials respectively. The tibialis anterior had similar cross correlation coefficients for the 26cm and 52cm trials examined, however, the 39cm condition showed very little cross correlation (-0.196 at 0.15s). The hamstring and soleus showed less of a correlation, 0.495 and 0.585 respectively (lag < 0.03) in the 26cm condition. The 39cm and 52cm trials produced low cross correlation in the hamstring and soleus as well.

The mean strains and strain rates (from Table 3) for this study increased in magnitude as the drop height increased. This trend is illustrated in Figures 8 and 9. The 26 cm landings produced the lowest strain and strain rates of the three conditions. The mean maximum principal strain produced by the 26 cm landing (595 ± 136 μstrain) was less than the 39 cm landing (879 ± 134.20 μstrain). Both the 26 and 39 cm landings resulted in less deformation (maximum principal) than the 52 cm condition (1077 ± 108 μstrain). The same trend appeared in the minimum principal strain data. However, minimum principle values become increasingly negative. The 26 cm landing (-593 ± 86 μstrain) produced a minimum principal strain less than the 39 cm landing (-645 ± 35

----------Insert Table 3 here----------

----------Insert Figure 8 here----------

μstrain). The 52 cm landing resulted in the greatest minimum principle strain (-769 ± 33

μstrain). Finally, the shear strain produced by the landings increased with height. Shear strain increased from 592 ± 111 μstrain to 760 ± 83 μstrain to 899 ± 98 μstrain each time the height increased.

The maximum principal strain rate increased as height increased. The 26 cm landing (8131 ± 2038 μstrain/s) resulted in a lower strain rate than the 39 cm landing (11668 ± 1292 μstrain/s) with the 52 cm landing having the greatest strain rate (14071 ± 3035 μstrain/s). The minimum principal strain rates in the 26 and 39 cm landings (-7500 ± 1265 μstrain/s and -7588 ± 310 μstrain/s respectively) were too similar to suggest a

----------Insert Figure 9 here----------

difference. However, the 52 cm landing resulted in greater minimum principal strain (-9570 ± 668 μstrain/s) than the other two heights. Maximum shear strain rate showed the same increasing trend. The 26 cm resulted in the lowest shear strain rate (7779 ± 1671 μstrain/s). The 39 cm landing shear strain rate (9591 ± 783 μstrain/s) was greater than the 26 cm but less than the 52 cm landing (11779 ± 1648 μstrain/s).

The mean maximum and minimum principal as well as the maximum shear strain were compared across all conditions using a Cohen's d effect size. Table 4 lists the effect

----------Insert Table 4 here----------

size for strain and strain rate comparisons between heights. The effect size calculation revealed large differences between strains at different landing heights for our subject. All of the comparisons except the strain rate in the 26cm and 39cm trials resulted in large effect size (ES > 0.8) [41].

DISCUSSION

The central goal in studying deformation patterns in bone in this study was to develop an understanding of stress fracture. A computational model was developed and used to simulate the drop landing movement. The influence of drop landing height on tibial deformation was examined. As the landing height increases, kinetic energy of the human body increases and as a result the lower extremities experience greater impact upon landing. We hypothesized that as the drop landing height increased, the tibial strain and strain rate would increase as well. Our hypothesis was supported. The maximum and minimum principal strain and the maximum shear strain increased with increased height. In addition, the maximum and minimum principal strain rates and the maximum shear strain rate also increased as drop landing height was increased.

The strain data reported here are lower than those previously reported [25]. Research evaluating various movements found *in vivo* strains during human movement between 400 and 2200 μstrain [22, 37, 43]. Ekenman et al. found an average strain of 2128 μstrain was produced in a female landing from a 45 cm height [37]. The subject in the present study experienced less tibial deformation when landing from a greater height. Milgrom et al. used an *in vivo* strain gauge technique to measure tibial deformation during landings from three different heights (26, 39, 52cm) and reported maximum principal tibial strains ranging from 896 to 1007 μstrain during landings from the same heights used in the present study [25]. Strains reported in the present study appeared lower than Milgrom's *in vivo* strain gauge study. In addition, the principal strain rates obtained in this study were much higher than those reported by Milgrom et al (Max Prin 4,796-7,621 μstrain/s, Min Prin 8,663-13,178 μstrain/s) [25]. However, shear strain rates were lower than Milgrom et al (24,493-50,890 μstrain/s).

While anthropometric differences exist between the subjects in this and previous studies, the primary difference was in footwear. The present study used a barefoot landing protocol, which may contribute to the differences in tibial strain and strain rates between the current study and previous research using footwear [13, 50]. Lanyon et al. performed an *in vivo* study that showed the affect of footwear on tibial strains [24]. Walking and running barefoot produced greater strain than when wearing shoes in Lanyon et al's study, which suggests that shoes have an effect on the strain experienced in the tibia. In the present study, it is possible that a strategy was chosen to protect the tibia from large strains. Milgrom et al. suggested a protective strategy was preferred by his subjects as well [25]. Future studies analyzing tibial deformation during drop landing should consider using footwear when performing the landing movement, so that results could be appropriately compared between *in vivo* and modeled strains.

The intent of this model was to, non-invasively, estimate tibial strain during drop landing. The accuracy of these estimations depends largely on the accuracy of the model. Comparison of measured versus simulated joint angle and muscle activation data resulted in strong correlation coefficients, which suggests that the model reasonably replicated the collected movement. The present study's strain fell below 1500 μstrain suggesting that the assumption regarding the bone's linear deformation was valid [35]. As a result of the calculated strains falling in the linear range of bone deformation and the good replication of the landing movement, it was concluded that the strain data derived from the computational model were reasonable.

The muscle activation similarities in 4 muscles (medial gastrocnemius, vastus medialis, vastus lateralis, and tibialis anterior) resulted in strong cross correlation

coefficients with the exception of the tibialis anterior in the 39cm trial. Variations in the simulated gastrocnemius and soleus patterns likely caused the change in the tibialis anterior pattern which shows little similarity to the measured tibialis anterior activity. These strong correlations suggest that a relationship exists between the two signals. However, the peak cross correlations occurred with phase shifts of varying magnitudes. The cause of the lag was not examined in this study but attempts should be made in future studies to determine an explanation for the lag. The muscles that displayed lower cross correlation coefficients (biceps femoris/lateral hamstring, and the soleus) were likely affected by coactivation, which was not accounted for in this nor previous models [26,27]. The models used in these studies are dependent on changes in muscle length to develop force. However, during isometric contraction, force is developed while the muscle length does not change [26].

The model used in this study displayed reasonable agreement with the actual, collected movement. This study demonstrated a reasonable solution to difficulties posed when measuring bone deformation with traditional *in vivo* methods has posed. Pairing musculoskeletal simulation with modal analysis creates a non-invasive method of examining tibial strain.

The flexible tibia was assumed to be transversly isotropic. The strain data from this study were below 1500 μstrain support the validity of this assumption. The right side of the model was actuated by 17 muscles, which is an improvement on previous models [26, 27]. However, marker data were retained from the right thigh cluster to create more desirable hip motion than the muscles alone could replicate. A model that replicated motion without the assistance of markers would be ideal.

The importance of this model is that the non-invasive method allows the incorporation of larger samples than *in vivo* deformation studies. In addition to drop landing, previous work has shown this method to be useful in examining tibial deformation during gait. It is possible that musculoskeletal models similar to this one could produce reasonable strain data during other movements as well. A number of movements in sport and military training can be examined closer to determine which produce the more dangerous strains. Modeling presents an opportunity to evaluate strain in bones inaccessible with implemented gauges such as the calcaneous.

In summary, drop landing height influenced tibial strains and strain rates in our subject. As the drop landing height increased, tibial strains and strain rates also increased. The computational modeling approach used in this study could yield reasonable tibial strain data that are within the reported ranges for human movement. The multibody dynamic simulation with a flexible tibia appears to be a valid approach to analyze tibial deformation during landing types of activities.

CONCLUSIONS

Drop landings have been evaluated using various biomechanical tools including motion capture and force plates. Previous research has sought to collect *in vivo* tibial strain data to provide insight on the development of stress fracture. The *in vivo* studies were admittedly small in scope as a result of reduced sample sizes. More recently, research involving musculoskeletal modeling has attempted to solve these shortcomings by examining modeled deformation with the intent of applying the model to larger

samples than previous studies. The present study was the first to attempt to examine bone strain during drop landings using the musculoskeletal modeling option.

Future research will focus on applying this model to a larger sample as well as examining other movements. The assumptions employed in this model can be examined closer. Controlling the hip joint and bi-articulate muscles is one area where simplifications were made in this model. Thigh markers controlled the hip joint in this study. Using a more complex muscle model may provide a more accurate model. The incorporation of physiological optimization in the muscles may create movements that are more accurate. The addition of tendons and ligaments will likely affect the tibial deformation. As with most applications of PID control, improving the tuning of the controllers should be examined in future research.

CONFLICT OF INTEREST

None of the authors have conflicts of interest.

ACKNOWLEDGEMENTS

This project was supported by DoD #W81XWH-08-1-0587 as well as an ASPiRE grant through the Ball State University Sponsored Programs Office. The authors would also like to thank Dan Leib and Scott Bergeon for their work developing the modeling process used here.

Table 1- Cross Correlation Coefficients and Lag between joint angles in one trial at each height

	26cm		39cm		52cm	
Joints	Cross Correlation Coefficient	Lag	Cross Correlation Coefficient	Lag	Cross Correlation Coefficient	Lag
Hip	0.87	0	0.94	0	0.906	0
Knee	0.996	-1	0.996	0	0.993	0
Ankle	0.996	0	0.998	0	0.996	0

Table 2- Cross Correlation Coefficients and Lag between muscle forces and EMG in one trial ate each height

	26cm		39cm		52cm	
Muscles	Cross Correlation Coefficient	Lag	Cross Correlation Coefficient	Lag	Cross Correlation Coefficient	Lag
Hams	0.495	3	0.374	-6	0.185	7
Gastroc	0.758	-12	0.700	-15	0.633	-11
VM	0.891	-6	0.860	-5	0.881	-6
VL	0.908	-8	0.825	-4	0.863	-5
Soleus	0.585	-2	0.403	-1	0.542	-3
TA	0.756	0	-0.196	-15	0.727	7

Table 3- Tibial Strain and Strain Rate derived from LifeMOD

Strain (µstrain)	26 cm		39 cm		52 cm	
	Mean	SD	Mean	SD	Mean	SD
Max Prin	595	136	879	134	1077	108
Min Prin	-593	86	-645	35	-769	33
Max Shear	592	111	760	83	899	98
Strain Rate (µstrain/s)						
Max Prin	8131	2038	11668	1292	14071	3035
Min Prin	-7500	1265	-7588	310	-9570	668
Max Shear	7779	1671	9591	783	11779	1648

Table 4- Cohen's d Effect Size comparing tibial deformation among drop heights

Strain	26 v 39	26 v 52	39 v 52
Max Prin	2.10	3.91	1.62
Min Prin	0.81	2.73	3.69
Max Shear	1.70	2.93	1.53
Strain Rate			
Max Prin	2.07	2.30	1.03
Min Prin	0.09	2.05	3.81
Max Shear	1.39	2.41	1.70

Figure 1- Musculoskeletal model used in the present study

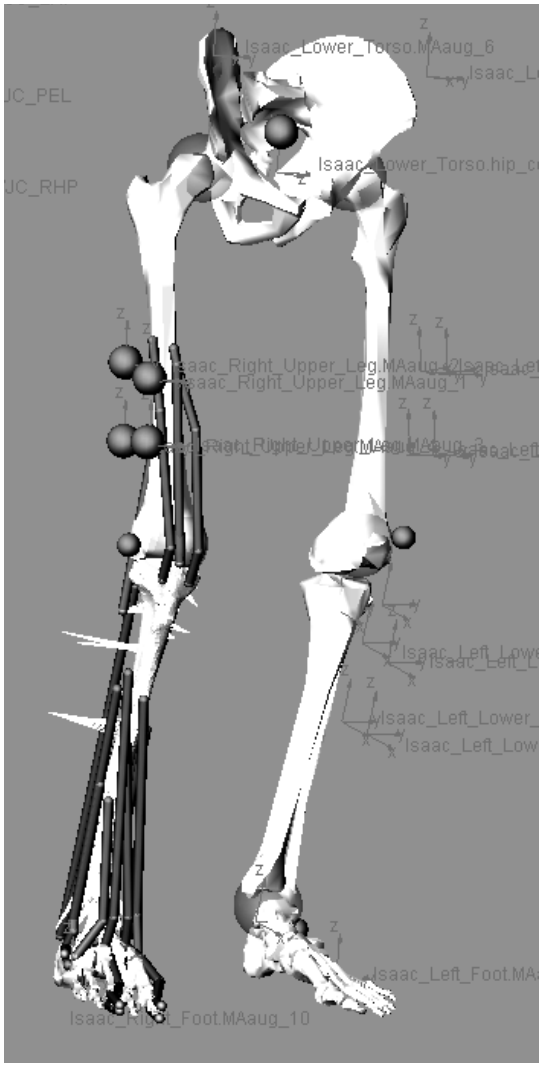

Figure 2- Joint angle comparisons (in degrees) between Visual 3D(—) and LifeMOD(---) for one 26 cm trial. Vertical line represents impact.

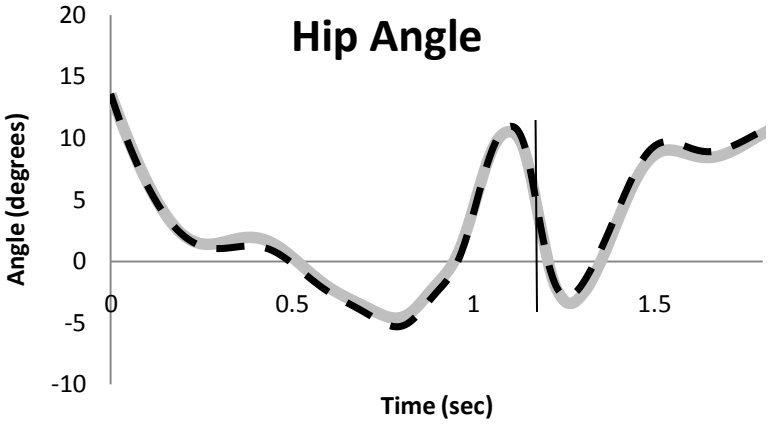

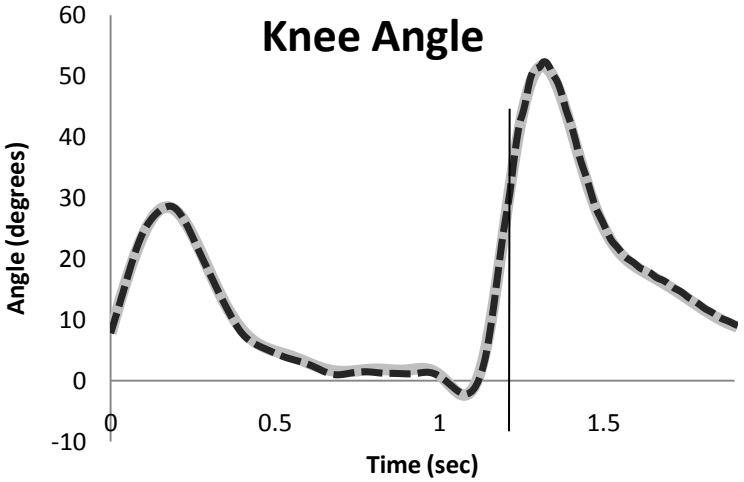

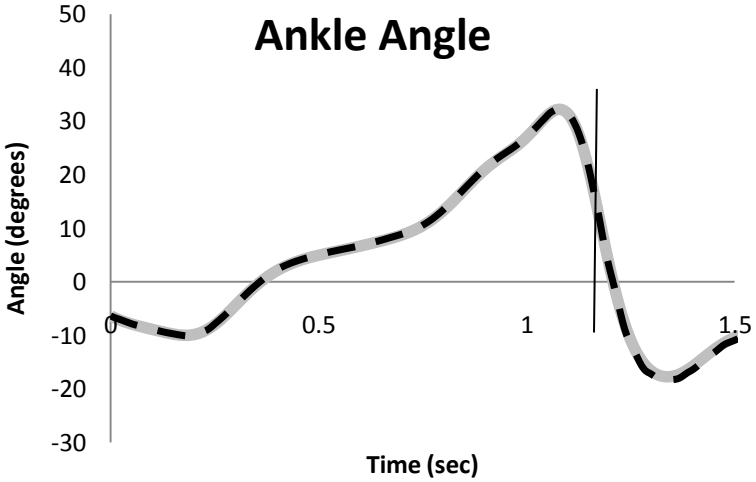

Figure 3- Joint angle comparisons (in degrees) between Visual 3D(—) and LifeMOD(---) for one 39 cm trial. Vertical line represents impact.

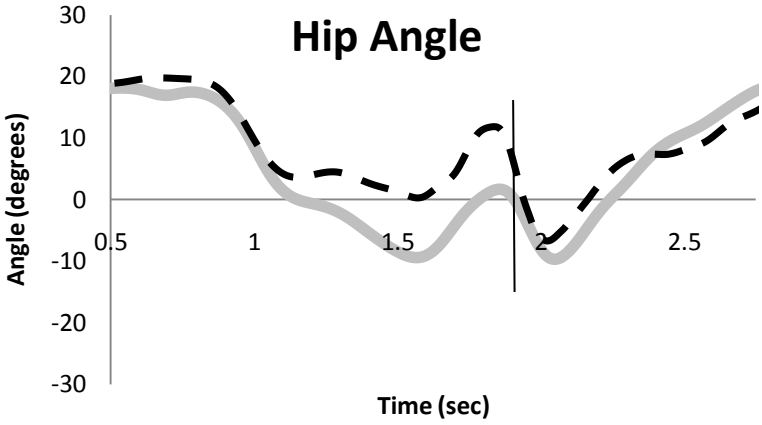

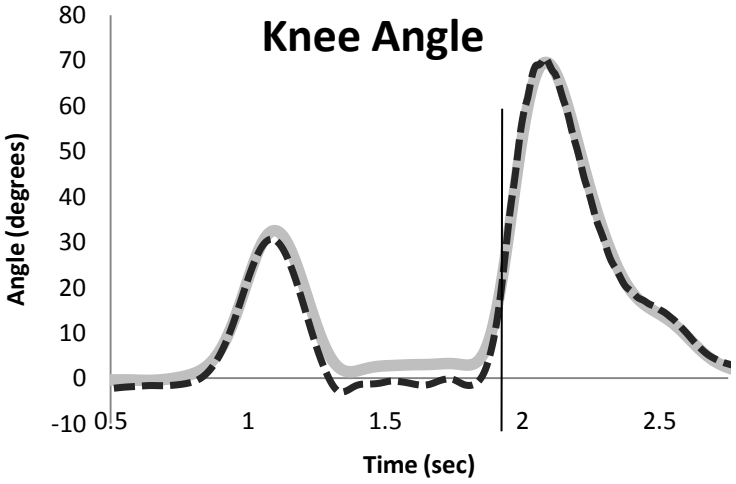

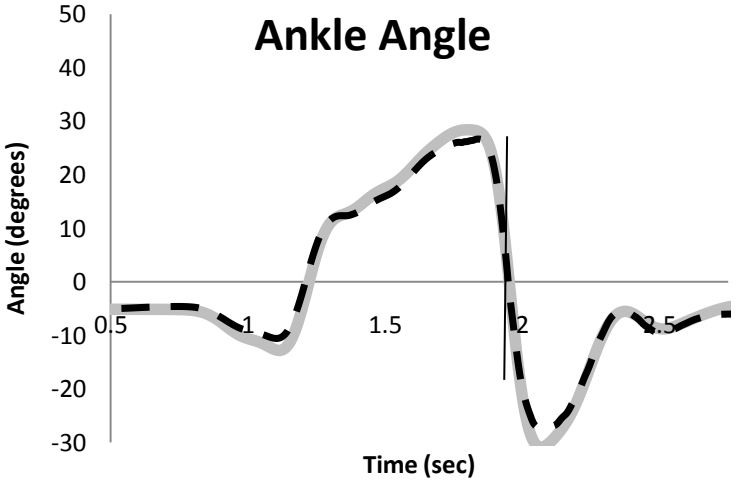

Figure 4- Joint angle comparisons (in degrees) between Visual 3D(—) and LifeMOD(---) for one 52 cm trial. Vertical line represents impact.

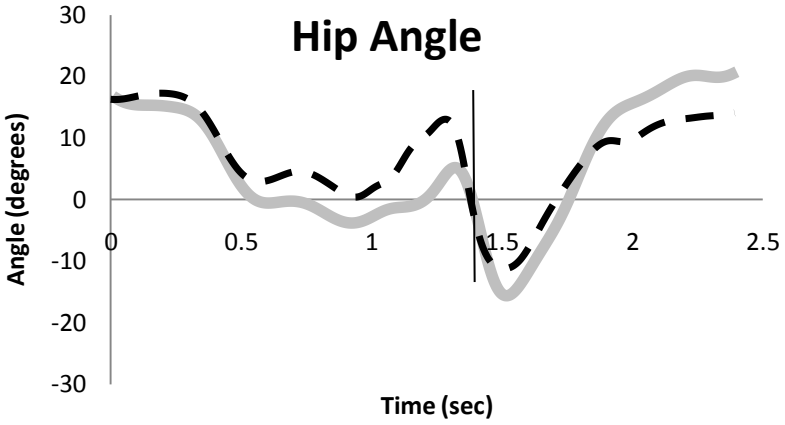

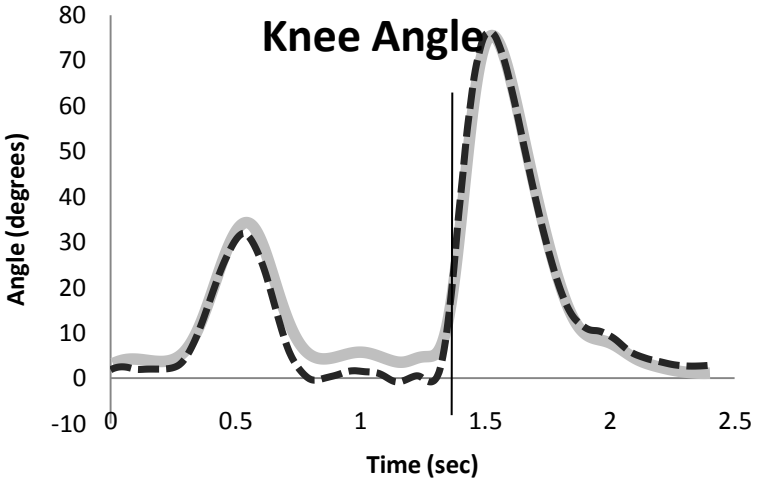

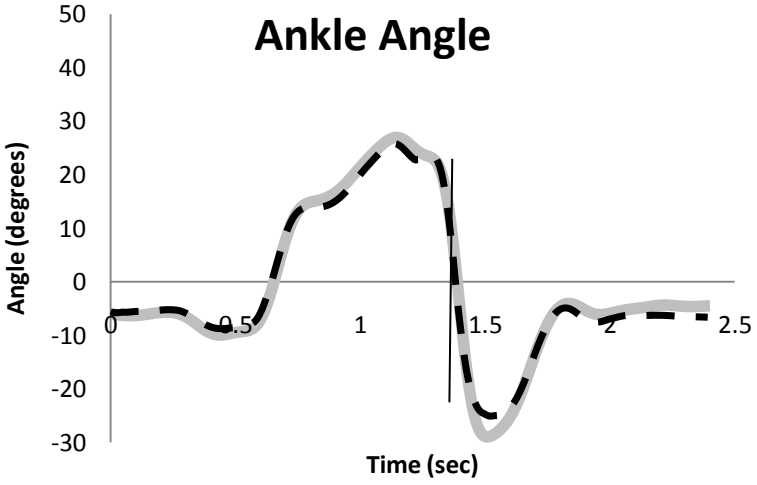

Figure 5- Normalized curves for measured EMG activity (---) and muscle force produced by the model (—) for one 26 cm trial. EMG and force data were normalized to the maximum value for each plot. VM: Vastus Medialis, VL: Vastus Lateralis, SOL: Soleus, RMG: Medial Gastrocnemius, TA: Tibialis Anterior, BF: Biceps Femoris (simulated force), RLH: Lateral Hamstring (measured EMG).

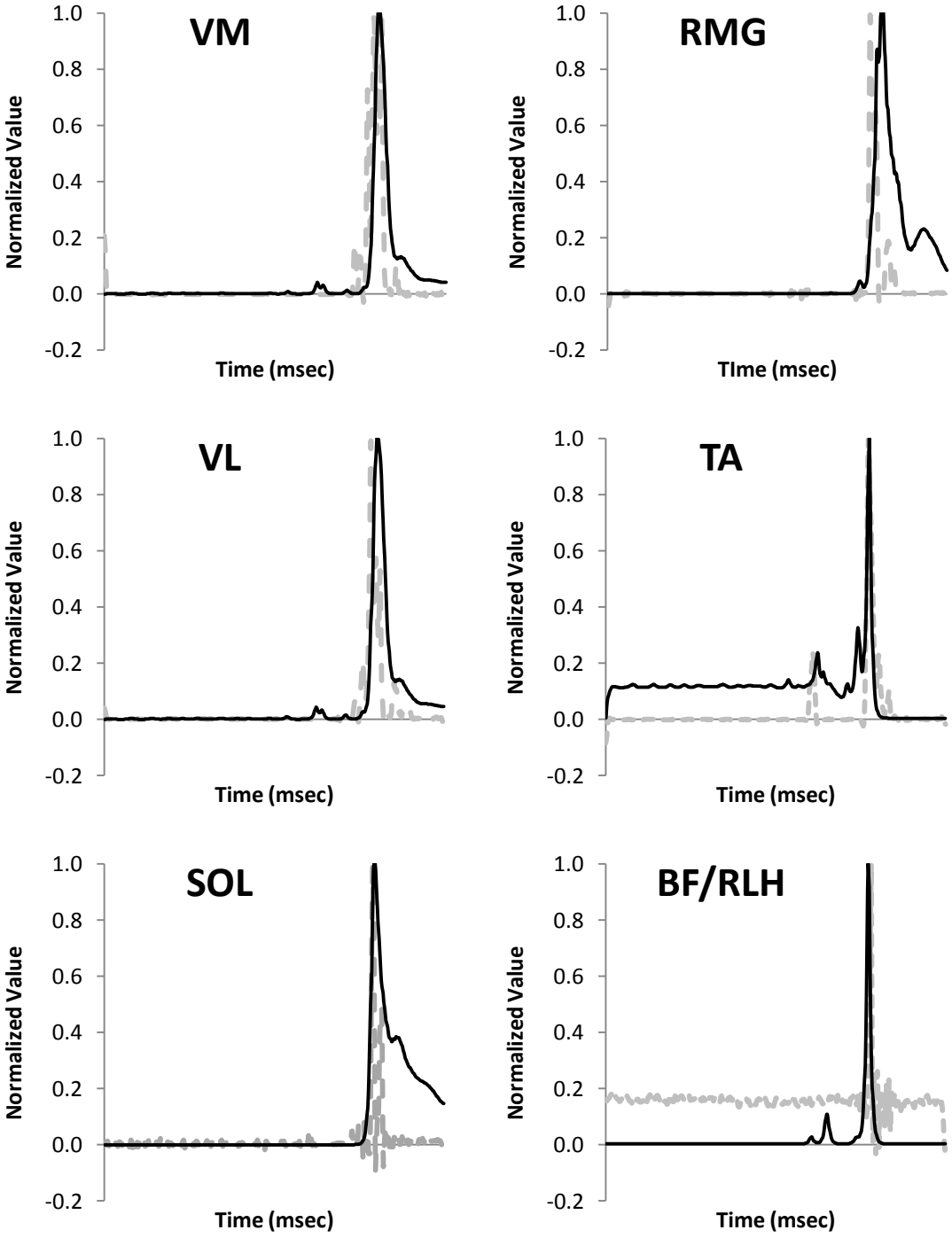

Figure 6- Normalized curves for measured EMG activity (---) and muscle force produced by the model (—) for one 39cm trial.

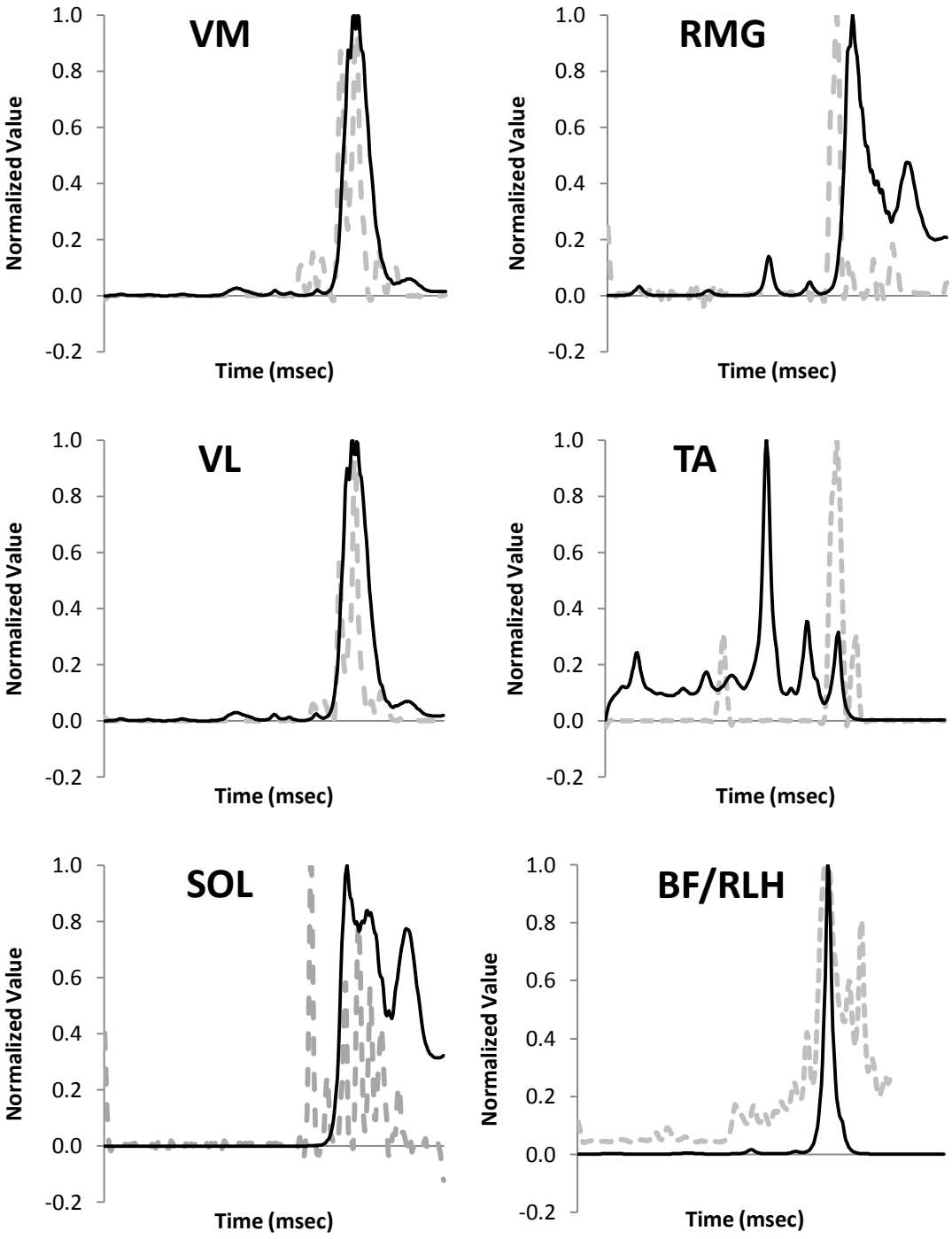

Figure 7- Normalized curves for measured EMG activity (---) and muscle force produced by the model (—) for one 52cm trial.

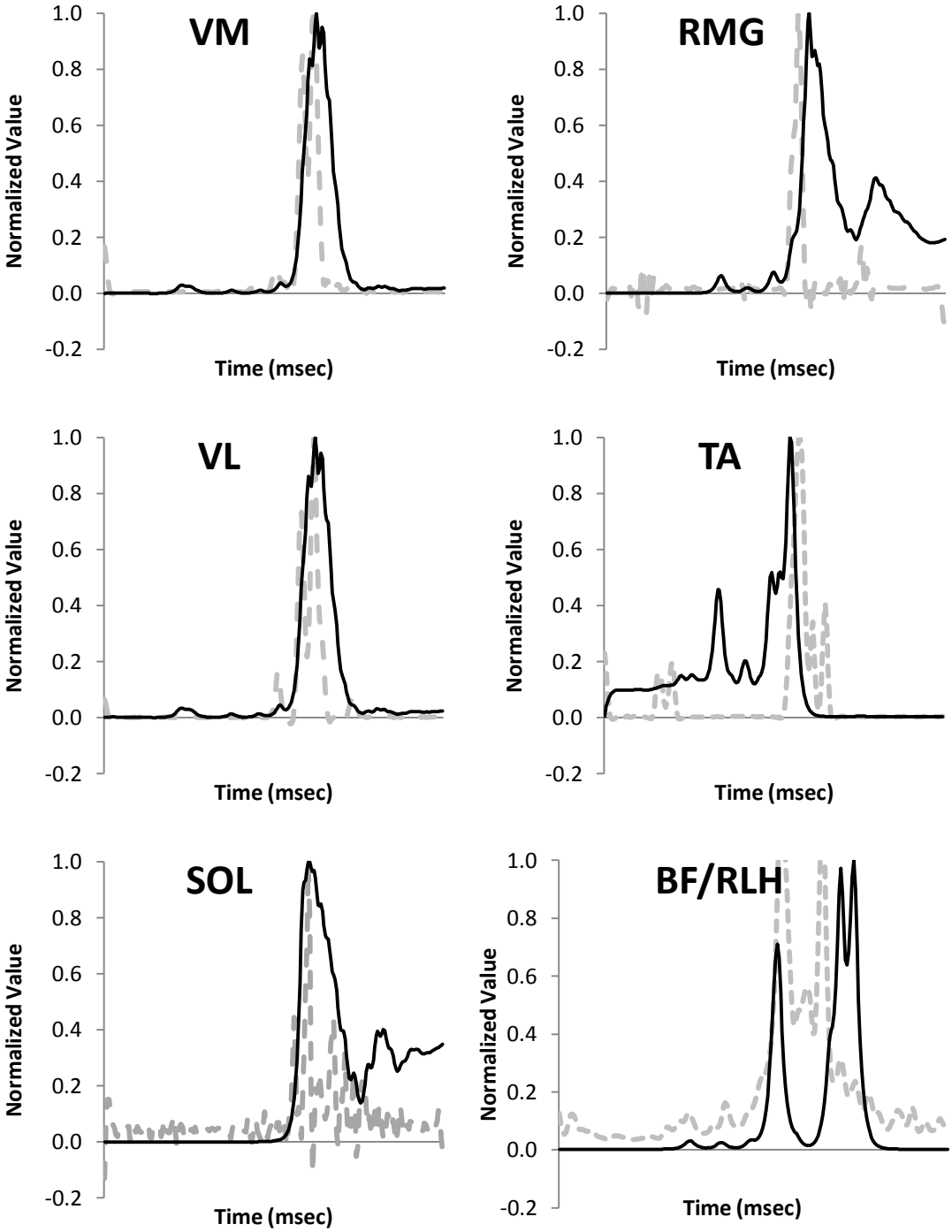

Figure 8- Strain produced from three landing heights.

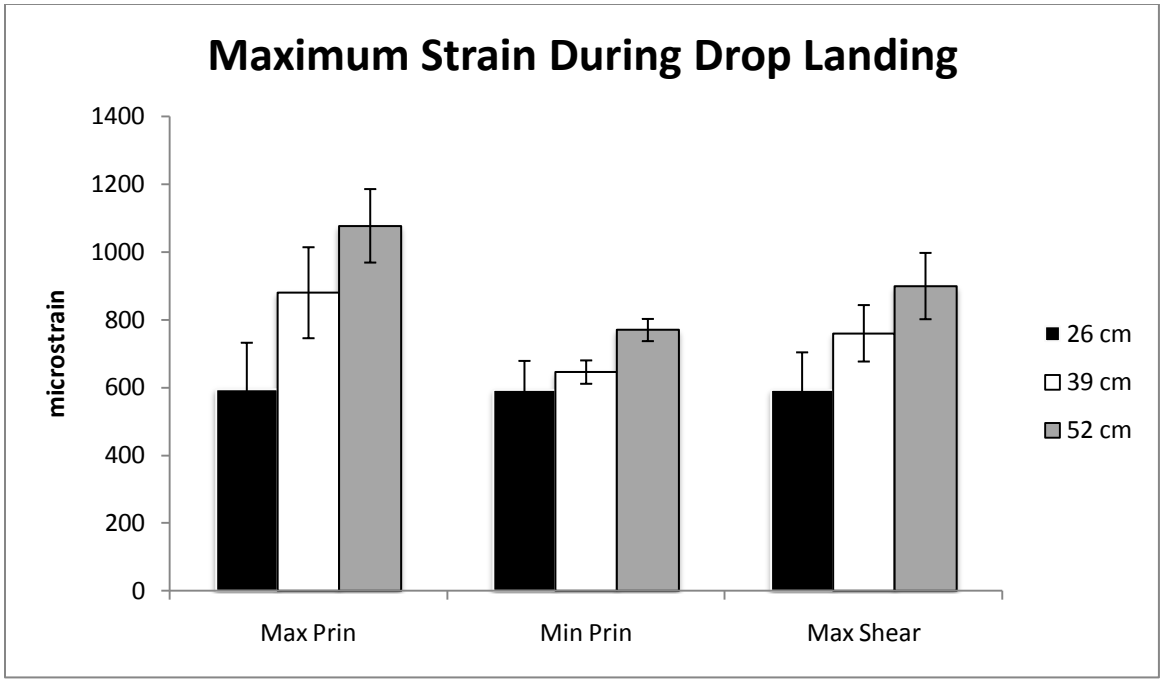

Figure 9- Strain rate produced from three landing heights.

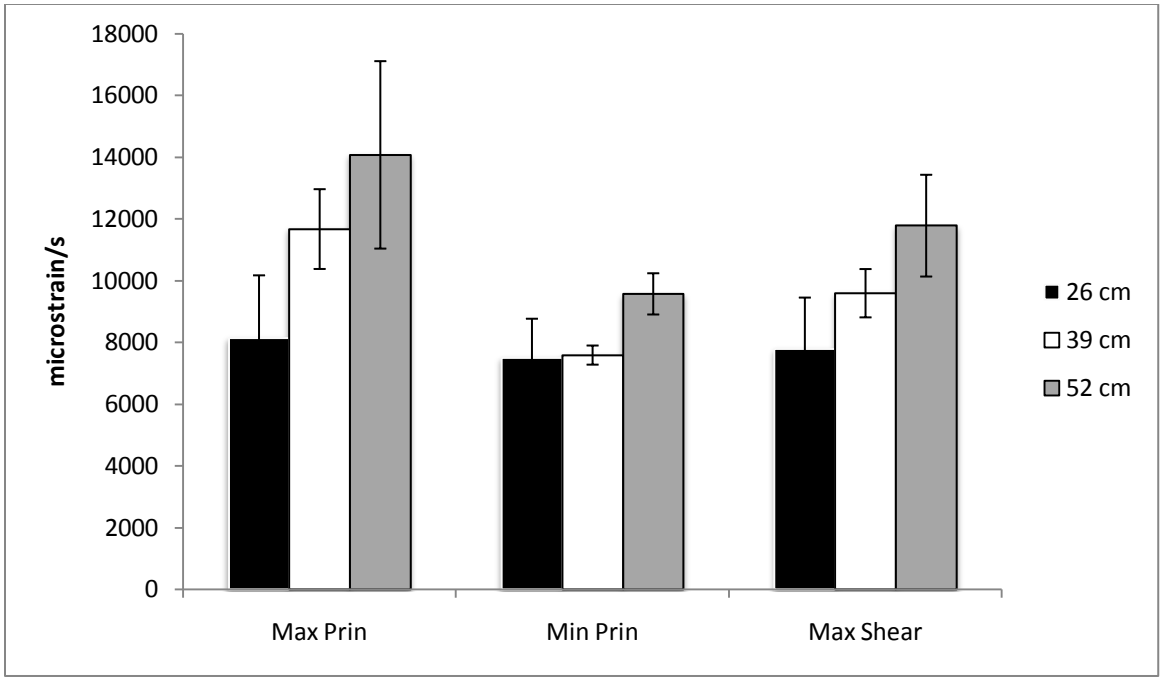

REFERENCES

1. Yeow, C.H., P.V.S. Lee, and J.C.H. Goh, *Effect of landing height on frontal plane kinematics, kinetics and energy dissipation at lower extremity joints.* Journal Of Biomechanics, 2009. **42**(12): p. 1967-1973.
2. Voloshin, A. and J. Wosk, *An in vivo study of low back pain and shock absorption in the human locomotor system.* J Biomech, 1982. **15**(1): p. 21-7.
3. Breithaupt, J.F., *Zur pathologie des mensch lichen fusses.* Med Ztg Berlin, 1855. **24**: p. 169-71, 175-77.
4. McBryde, A.M., Jr., *Stress fractures in athletes.* J Sports Med, 1975. **3**(5): p. 212-7.
5. Armstrong, D.W., 3rd, et al., *Stress fracture injury in young military men and women.* Bone, 2004. **35**(3): p. 806-16.
6. Meyer, S.A., C.L. Saltzman, and J.P. Albright, *Stress fractures of the foot and leg.* Clin Sports Med, 1993. **12**(2): p. 395-413.
7. Milgrom, C., et al., *An analysis of the biomechanical mechanism of tibial stress fractures among Israeli infantry recruits. A prospective study.* Clin Orthop Relat Res, 1988(231): p. 216-21.
8. Shaffer, R.A., et al., *Use of simple measures of physical activity to predict stress fractures in young men undergoing a rigorous physical training program.* American Journal of Epidemiology, 1999. **149**(3): p. 236-242.
9. Matheson, G.O., et al., *Stress fractures in athletes. A study of 320 cases.* Am J Sports Med, 1987. **15**(1): p. 46-58.
10. Dixon, M. and P. Fricker, *Injuries to elite gymnasts over 10 yr.* Med Sci Sports Exerc, 1993. **25**(12): p. 1322-9.
11. Frusztajer, N.T., et al., *Nutrition and the incidence of stress fractures in ballet dancers.* Am J Clin Nutr, 1990. **51**(5): p. 779-83.
12. Goldberg, B. and C. Pecora, *Stress fractures: a risk of increased training in freshman.* Physician and Sportsmedicine, 1994. **22**: p. 68-78.
13. Johnson, A.W., C.B. Weiss, Jr., and D.L. Wheeler, *Stress fractures of the femoral shaft in athletes--more common than expected. A new clinical test.* Am J Sports Med, 1994. **22**(2): p. 248-56.
14. Kadel, N.J., C.C. Teitz, and R.A. Kronmal, *Stress fractures in ballet dancers.* Am J Sports Med, 1992. **20**(4): p. 445-9.
15. Pecina, M., I. Bojanic, and S. Dubravcic, *Stress fractures in figure skaters.* Am J Sports Med, 1990. **18**(3): p. 277-9.
16. Warren, M.P., et al., *Scoliosis and fractures in young ballet dancers. Relation to delayed menarche and secondary amenorrhea.* N Engl J Med, 1986. **314**(21): p. 1348-53.
17. Brukner, P., et al., *Stress fractures: a review of 180 cases.* Clin J Sport Med, 1996. **6**(2): p. 85-9.
18. Milgrom, C., et al., *Stress fractures in military recruits. A prospective study showing an unusually high incidence.* J Bone Joint Surg Br, 1985. **67**(5): p. 732-5.
19. Frost, H.M., *Why do marathon runners have less bone than weight lifters? A vital-biomechanical view and explanation.* Bone, 1997. **20**(3): p. 183-189.
20. Fredericson, M., et al., *Stress fractures in athletes.* Top Magn Reson Imaging, 2006. **17**(5): p. 309-25.
21. Li, G.P., et al., *Radiographic and histologic analyses of stress fracture in rabbit tibias.* Am J Sports Med, 1985. **13**(5): p. 285-94.
22. Burr, D.B., et al., *In vivo measurement of human tibial strains during vigorous activity*. Bone, 1996. **18**(5): p. 405-410.
23. Ekenman, I., et al., *The reliability and validity of an instrumented staple system for in vivo measurement of local bone deformation. An in vitro study.* Scand J Med Sci Sports, 1998. **8**(3): p. 172-6.
24. Lanyon, L.E., et al., *Bone deformation recorded in vivo from strain gauges attached to the human tibial shaft.* Acta Orthop Scand, 1975. **46**(2): p. 256-68.
25. Milgrom, C., et al., *Do high impact exercises produce higher tibial strains than running?* Br J Sports Med, 2000. **34**(3): p. 195-9.
26. Al Nazer, R., et al., *Flexible multibody simulation approach in the analysis of tibial strain during walking.* Journal Of Biomechanics, 2008. **41**(5): p. 1036-1043.

27. Al Nazer, R., et al., *Analysis of dynamic strains in tibia during human locomotion based on flexible multibody approach integrated with magnetic resonance imaging technique.* Multibody System Dynamics, 2008. **20**(4): p. 287-306.
28. *LifeMOD 2008.0 Online Manual*. 2008 [cited 2010 March 8]; 2008.0:[The online manual and guide for LifeMOD 2008]. Available from: http://www.lifemodeler.com/LM_Manual/index.shtml.
29. Johnson, M.A., M.H. Moradi, and J. Crowe, *PID control : new identification and design methods*. 2005, New York: Springer. xxvii, 543 p.
30. Shabana, A.A., *Dynamics of multibody systems*. 2nd ed. 1998, Cambridge, U.K. ; New York: Cambridge University Press. xii, 372 p.
31. Schwartz, M.H. and A. Rozumalski, *A new method for estimating joint parameters from motion data.* J Biomech, 2005. **38**(1): p. 107-16.
32. Cram, J.R.K.G.S.H.J.P.G.M.A.P.Y.D.x.p.i. and cm, eds. *Introduction to surface electromyography*. 1998, Aspen Publishers: Gaithersburg, Md. 408.
33. Dong, X.N. and X.E. Guo, *The dependence of transversely isotropic elasticity of human femoral cortical bone on porosity.* J Biomech, 2004. **37**(8): p. 1281-7.
34. Schileo, E., et al., *Subject-specific finite element models can accurately predict strain levels in long bones.* J Biomech, 2007. **40**(13): p. 2982-9.
35. Pattin, C.A., W.E. Caler, and D.R. Carter, *Cyclic mechanical property degradation during fatigue loading of cortical bone.* J Biomech, 1996. **29**(1): p. 69-79.
36. Craig, R.R. and M.C.C. Bampton, *Coupling of substructures for dynamic analysis.* American Institute of Aeronautics and Astronautics Journal, 1968. **6**: p. 1313-1319.
37. Ekenman, I., et al., *Local bone deformation at two predominant sites for stress fractures of the tibia: an in vivo study.* Foot Ankle Int, 1998. **19**(7): p. 479-84.
38. Turner, C.H., et al., *High frequency components of bone strain in dogs measured during various activities.* J Biomech, 1995. **28**(1): p. 39-44.
39. *Cross-correlation Analysis of Filtered and Rectified Waveforms*. SCRC Data Capture and Analysis Software Tutorials [cited 2010 March 22]; Available from: http://www.scrc.umanitoba.ca/doc/tutorial/T14_crosscorr_filtered_wfs.doc.
40. Yaffee, R.A. and M. McGee, *Introduction to time series analysis and forecasting : with applications in SAS and SPSS*. 2000, San Diego: Academic Press. xxv, 528 p.
41. Cohen, J., *A power primer.* Psychol Bull, 1992. **112**(1): p. 155-9.
42. Nakagawa, S. and I.C. Cuthill, *Effect size, confidence interval and statistical significance: a practical guide for biologists.* Biol Rev Camb Philos Soc, 2007. **82**(4): p. 591-605.
43. Milgrom, C., et al., *In-vivo strain measurements to evaluate the strengthening potential of exercises on the tibial bone.* J Bone Joint Surg Br, 2000. **82**(4): p. 591-4.

CHAPTER 5

SUMMARY AND CONCLUSIONS

SUMMARY

The purpose of this study was to develop a computational model to measure strain and strain rate in the tibia while landing from various heights. It was hypothesized that this model would accurately simulate human movement patterns and calculate deformation in the tibia. The strain produced by human movement has been studied in an effort to answer questions regarding stress fracture development. Two studies have used *in vivo* strain measurement in animals [64, 72] to evaluate bone strain during various movements. Lanyon's research first demonstrated the use of *in vivo* strain measurement

in humans [12]. However, studies using *in vivo* strain measurement have struggled to collect data on more than a small sample often consisting of members from their own research team [8, 11-14, 16, 37, 45]. Musculoskeletal models have been developed for simulating human movement with the ultimate goal of replicating bone strain. The non-invasive methodology allows for larger cohorts to be recruited.

The method used here is a combination of FEA and MBD. The movement was first simulated using LifeMOD. The FEM tibia was developed in Marc and inserted into the model in LifeMOD. The research team was able to extract the strain values and run the subsequent statistical tests to form the results. Our subject experienced increasing amounts of strain as the landing height increased. The effect size showed that the differences in strain for each height were large according to Cohen's guidelines [70]. All but one comparison revealed effect sizes greater than 0.8.

CONCLUSIONS

Computational models are simplifications of complex, real-world, events. The computational cost to create exact replications of these events is too great and the knowledge does not exist to build such a model. The goal of researchers in this area is twofold. The first goal is to continue to improve models from their crude or oversimplified state to an ideal simulation. The second goal should be to apply the model to functional situations. While assumptions were made in this model, we sought to fulfill these two requirements. Improvements were made to previous models by using a subject

specific geometry when developing the flexible tibia. The functional application was to examine the tibial deformation during the landing which prior to this study required invasive procedures.

The strain and strain rate recorded in this study were on the low end of the acceptable range reported by numerous *in vivo* studies. We believe that a few factors contributed to these variations. The use of shoes in previous studies likely attributed to the differences. In an effort to eliminate the possible variability between subjects (for future studies), this study performed the movements barefoot. As a result, the variation in footwear was a limitation in comparing our findings to those of previous researchers.

While the data from this study fell into accepted ranges, the strain ad strain rates were much lower than previously reported by Milgrom et al [10]. While anthropometric differences exist between the subject in this and subjects in previous studies, the primary difference was in footwear [10, 36]. The present study performed landings barefoot, which appear to have resulted in landing strategy differences. Landing strategy contributes significantly to the forces acting upon skeletal system[42]. This is a limiting factor when comparing studies because there the literature to explain precisely how footwear affects tibial strains is lacking. It is intuitive that being barefoot would have an effect on the tibial strain during landing. The Lanyon et al. work investigated the effect of shoes on tibial strain using the *in vivo* method. Barefoot running and walking produced greater strain compared to shod conditions [12]. Al Nazer's simulation resulted in greater strain than Lanyon's despite the lack of footwear. Both findings would support increased strain in our simulation. However, the present study resulted in reduced strain

data compared to Milgrom's shod *in vivo* study [10]. We suspect that the subject in the present study employed a strategy that favored the protection of the skeletal system as result of being barefoot. Comparison between barefoot and shod conditions while landing are necessary to confirm these ideas. Further research explicitly aimed at understanding the effect of footwear on tibial strains is needed.

The comparison in joint angles and muscle forces suggest that our model reasonably simulated the landing movement. Joint angle (hip, knee, ankle) comparisons yielded cross correlation coefficients that suggest strong correlations at small lags (>0.01s). In addition, comparisons of the activity in six muscles yielded cross correlation coefficients that suggest strong correlation between simulated muscle force and measured EMG existed. The maximum cross correlation coefficients for the muscle activity occurred at varying lags (-0.15-0.07s). The presence of lag in the signal needs to be examined more closely. The cause of the lag was not examined in this study but attempts should be made in future studies to determine an explanation for the lag. It is possible that the lag is a result of comparing simulated muscle forces to measured activations. Future research should consider comparing measured EMG to the simulated muscle activity instead. This analysis may produce results that are more favorable. The muscles that displayed lower cross correlation coefficients (biceps femoris/lateral hamstring, and the soleus) were likely affected by coactivation, which was not accounted for in this nor previous models [2, 73]. The model used in these studies is dependent on changes in length of muscles to develop force. In isometric contraction, for example, force is developed while the muscle length does not change [2].

Other factors that may affect bone fragility have been identified including nutrition, genetics, hormonal influence, and muscle strength [7]. These factures were outside of the scope of this project and were not analyzed in this study. Previous studies have used samples consisting of older participants than our subject [10]. Milgrom et al. analyzed strain data in subjects aged 27 to 52 years. Males and females participated in Milgrom's study. The affect gender has on bone deformation is not yet fully understood but is generally accepted as playing some part. Again, the gender difference may have played a role in strain differences.

RECOMMENDATIONS FOR FUTURE RESEARCH

Future research can focus in a few areas. The usefulness of this model is the ability to evaluate strains in a larger sample than previous *in vivo* studies. Now that this model has been developed, we hope to apply it to a larger sample of subjects. This model made assumptions that future models could improve on. Controlling the hip joint and bi-articulate muscles is one area where simplifications were made. Future research should focus on improving the muscles used in this study. The incorporation of physiological optimization in the muscles may create movements more accurately representing that of a human's. This and previous models ignored the musculotendenous attachments by attaching the muscles directly to the flexible tibia. The addition of tendons and ligaments will likely affect the tibial deformation. As with most applications of PID control, improving the tuning of the controllers should be examined in future research.

CHAPTER 6

REFERENCES

1. Yeow, C.H., P.V.S. Lee, and J.C.H. Goh, *Effect of landing height on frontal plane kinematics, kinetics and energy dissipation at lower extremity joints.* Journal Of Biomechanics, 2009. **42**(12): p. 1967-1973.
2. Al Nazer, R., et al., *Flexible multibody simulation approach in the analysis of tibial strain during walking.* Journal Of Biomechanics, 2008. **41**(5): p. 1036-1043.
3. Wosk, J. and A. Voloshin, *Wave attenuation in skeletons of young healthy persons.* J Biomech, 1981. **14**(4): p. 261-7.
4. Scott, S.H. and D.A. Winter, *Internal forces of chronic running injury sites.* Med Sci Sports Exerc, 1990. **22**(3): p. 357-69.
5. Stanitski, C.L., J.H. McMaster, and P.E. Scranton, *On the nature of stress fractures.* Am J Sports Med, 1978. **6**(6): p. 391-6.
6. Li, G.P., et al., *Radiographic and histologic analyses of stress fracture in rabbit tibias.* Am J Sports Med, 1985. **13**(5): p. 285-94.
7. Brukner, P., B. Kim, and M. Gordon, *Stress fractures*. 1999, Vic., Australia : Blackwell Science Asia: Champaign, IL. xi, 190 p.
8. Mendelson, S., et al., *Effect of cane use on tibial strain and strain rates.* American Journal of Physical Medicine & Rehabilitation, 1998. **77**(4): p. 333-338.
9. Meyer, S.A., C.L. Saltzman, and J.P. Albright, *Stress fractures of the foot and leg.* Clin Sports Med, 1993. **12**(2): p. 395-413.
10. Milgrom, C., et al., *Do high impact exercises produce higher tibial strains than running?* Br J Sports Med, 2000. **34**(3): p. 195-9.
11. Burr, D.B., et al., *In vivo measurement of human tibial strains during vigorous activity.* Bone, 1996. **18**(5): p. 405-410.
12. Lanyon, L.E., et al., *Bone deformation recorded in vivo from strain gauges attached to the human tibial shaft.* Acta Orthop Scand, 1975. **46**(2): p. 256-68.
13. Milgrom, C., et al., *The effect of shoe sole composition on in vivo tibial strains during walking.* Foot Ankle Int, 2001. **22**(7): p. 598-602.
14. Milgrom, C., et al., *In-vivo strain measurements to evaluate the strengthening potential of exercises on the tibial bone.* J Bone Joint Surg Br, 2000. **82**(4): p. 591-4.
15. Milgrom, C., et al., *An analysis of the biomechanical mechanism of tibial stress fractures among Israeli infantry recruits. A prospective study.* Clin Orthop Relat Res, 1988(231): p. 216-21.
16. Milgrom, C., et al., *The effect of muscle fatigue on in vivo tibial strains.* J Biomech, 2007. **40**(4): p. 845-50.
17. Miles, A.W. and K.E. Tanner, *Strain measurement in biomechanics*. 1st ed. 1992, London ; New York: Chapman & Hall. xiv, 191 p.
18. Breithaupt, J.F., *Zur pathologie des mensch lichen fusses.* Med Ztg Berlin, 1855. **24**: p. 169-71, 175-77.
19. McBryde, A.M., Jr., *Stress fractures in athletes.* J Sports Med, 1975. **3**(5): p. 212-7.
20. Armstrong, D.W., 3rd, et al., *Stress fracture injury in young military men and women.* Bone, 2004. **35**(3): p. 806-16.
21. Shaffer, R.A., et al., *Use of simple measures of physical activity to predict stress fractures in young men undergoing a rigorous physical training program.* American Journal of Epidemiology, 1999. **149**(3): p. 236-242.
22. Matheson, G.O., et al., *Stress fractures in athletes. A study of 320 cases.* Am J Sports Med, 1987. **15**(1): p. 46-58.

23. Goldberg, B. and C. Pecora, *Stress fractures: a risk of increased training in freshman.* Physician and Sportsmedicine, 1994. **22**: p. 68-78.
24. Johnson, A.W., C.B. Weiss, Jr., and D.L. Wheeler, *Stress fractures of the femoral shaft in athletes--more common than expected. A new clinical test.* Am J Sports Med, 1994. **22**(2): p. 248-56.
25. Dixon, M. and P. Fricker, *Injuries to elite gymnasts over 10 yr.* Med Sci Sports Exerc, 1993. **25**(12): p. 1322-9.
26. Pecina, M., I. Bojanic, and S. Dubravcic, *Stress fractures in figure skaters.* Am J Sports Med, 1990. **18**(3): p. 277-9.
27. Frusztajer, N.T., et al., *Nutrition and the incidence of stress fractures in ballet dancers.* Am J Clin Nutr, 1990. **51**(5): p. 779-83.
28. Kadel, N.J., C.C. Teitz, and R.A. Kronmal, *Stress fractures in ballet dancers.* Am J Sports Med, 1992. **20**(4): p. 445-9.
29. Warren, M.P., et al., *Scoliosis and fractures in young ballet dancers. Relation to delayed menarche and secondary amenorrhea.* N Engl J Med, 1986. **314**(21): p. 1348-53.
30. Hickey, G.J., P.A. Fricker, and W.A. McDonald, *Injuries of young elite female basketball players over a six-year period.* Clin J Sport Med, 1997. **7**(4): p. 252-6.
31. Brukner, P., et al., *Stress fractures: a review of 180 cases.* Clin J Sport Med, 1996. **6**(2): p. 85-9.
32. Milgrom, C., et al., *Stress fractures in military recruits. A prospective study showing an unusually high incidence.* J Bone Joint Surg Br, 1985. **67**(5): p. 732-5.
33. Milgrom, C., *The Israeli elite infantry recruit: a model for understanding the biomechanics of stress fractures.* J R Coll Surg Edinb, 1989. **34**(6 Suppl): p. S18-22.
34. Frost, H.M., *Why do marathon runners have less bone than weight lifters? A vital-biomechanical view and explanation.* Bone, 1997. **20**(3): p. 183-189.
35. Frost, H.M., *On our age-related bone loss: insights from a new paradigm.* J Bone Miner Res, 1997. **12**(10): p. 1539-46.
36. Ekenman, I., et al., *Local bone deformation at two predominant sites for stress fractures of the tibia: an in vivo study.* Foot Ankle Int, 1998. **19**(7): p. 479-84.
37. Milgrom, C., et al., *A home exercise program for tibial bone strengthening based on in vivo strain measurements.* Am J Phys Med Rehabil, 2001. **80**(6): p. 433-8.
38. Mow, V.C. and R. Huiskes, *Basic orthopaedic biomechanics & mechano-biology*. 3rd ed. 2005, Philadelphia, PA: Lippincott Williams & Wilkins. p.
39. Fredericson, M., et al., *Stress fractures in athletes.* Top Magn Reson Imaging, 2006. **17**(5): p. 309-25.
40. Johansson, C., I. Ekenman, and R. Lewander, *Stress fracture of the tibia in athletes: diagnosis and natural course.* Scandinavian Journal of Medicine & Science in Sports, 1992. **2**(2): p. 87-91.
41. Voloshin, A. and J. Wosk, *An in vivo study of low back pain and shock absorption in the human locomotor system.* J Biomech, 1982. **15**(1): p. 21-7.
42. Seegmiller, J.G. and S.T. McCaw, *Ground Reaction Forces Among Gymnasts and Recreational Athletes in Drop Landings.* J Athl Train, 2003. **38**(4): p. 311-314.
43. Hibbeler, R.C., *Engineering mechanics. Statics and dynamics*. 11th ed. 2007, Upper Saddle River, N.J.: Pearson/Prentice-Hall. xvi, 718 p.
44. Fyhrie, D.P., et al., *Effect of fatiguing exercise on longitudinal bone strain as related to stress fracture in humans.* Annals of Biomedical Engineering, 1998. **26**(4): p. 660-665.

45. Milgrom, C., et al., *A comparison of the effect of shoes on human tibial axial strains recorded during dynamic loading.* Foot Ankle Int, 1998. **19**(2): p. 85-90.
46. Milgrom, C., et al., *Are overground or treadmill runners more likely to sustain tibial stress fracture?* Br J Sports Med, 2003. **37**(2): p. 160-3.
47. Milgrom, C., et al., *Using bone's adaptation ability to lower the incidence of stress fractures.* American Journal of Sports Medicine, 2000. **28**(2): p. 245-251.
48. Schileo, E., et al., *Subject-specific finite element models implementing a maximum principal strain criterion are able to estimate failure risk and fracture location on human femurs tested in vitro.* J Biomech, 2008. **41**(2): p. 356-67.
49. Schileo, E., et al., *Subject-specific finite element models can accurately predict strain levels in long bones.* J Biomech, 2007. **40**(13): p. 2982-9.
50. Ekenman, I., et al., *The reliability and validity of an instrumented staple system for in vivo measurement of local bone deformation. An in vitro study.* Scand J Med Sci Sports, 1998. **8**(3): p. 172-6.
51. Cheung, J.T., et al., *Three-dimensional finite element analysis of the foot during standing--a material sensitivity study.* J Biomech, 2005. **38**(5): p. 1045-54.
52. Pattin, C.A., W.E. Caler, and D.R. Carter, *Cyclic mechanical property degradation during fatigue loading of cortical bone.* J Biomech, 1996. **29**(1): p. 69-79.
53. Craig, R.R. and M.C.C. Bampton, *Coupling of substructures for dynamic analysis.* American Institute of Aeronautics and Astronautics Journal, 1968. **6**: p. 1313-1319.
54. Shabana, A.A., *Dynamics of multibody systems*. 2nd ed. 1998, Cambridge, U.K. ; New York: Cambridge University Press. xii, 372 p.
55. Ang, K.H., C. G.C.Y, and Y. Li, *PID control system analysis, design, and technology.* IEEE Transactionson Control Systems, 2005. **13**(4): p. 559-576.
56. Johnson, M.A., M.H. Moradi, and J. Crowe, *PID control : new identification and design methods*. 2005, New York: Springer. xxvii, 543 p.
57. Cram, J.R.K.G.S.H.J.P.G.M.A.P.Y.D.x.p.i. and cm, eds. *Introduction to surface electromyography*. 1998, Aspen Publishers: Gaithersburg, Md. 408.
58. Schwartz, M.H. and A. Rozumalski, *A new method for estimating joint parameters from motion data.* J Biomech, 2005. **38**(1): p. 107-16.
59. O'Brien, J.F., et al. *Automatic Joint Parameter Estimation from Magnetic Motion Capture Data*. in *Proceedings of Graphics Interface*. 2000.
60. Dong, X.N. and X.E. Guo, *The dependence of transversely isotropic elasticity of human femoral cortical bone on porosity.* J Biomech, 2004. **37**(8): p. 1281-7.
61. *LifeMOD 2008.0 Online Manual*. 2008 [cited 2010 March 8]; 2008.0:[The online manual and guide for LifeMOD 2008]. Available from: http://www.lifemodeler.com/LM_Manual/index.shtml.
62. Hall, I.H., *Deformation of solids*. 1968, New York,: Barnes & Noble. ix, 227 p.
63. Clanton, T., *Prophylactic ankle stabilizers and their effect on lower extremity landing mechanics during drop jump landings to fatigue*, in *School of Physical Education, Sport, and Exercise Science*. 2009, Ball State University: Muncie. p. 92.
64. Turner, C.H., et al., *High frequency components of bone strain in dogs measured during various activities.* J Biomech, 1995. **28**(1): p. 39-44.
65. Hinton, O. *Digital Signal Processing*. Chapter 6: Describing Random Sequences [PDF] 2001 6/23/2010]; Available from: http://www.staff.ncl.ac.uk/oliver.hinton/eee305/Chapter6.pdf.

66. Box, G.E.P., G.M. Jenkins, and G.C. Reinsel, *Time series analysis : forecasting and control*. 4th ed. Wiley series in probability and statistics. 2008, Hoboken, N.J.: John Wiley. xxiv, 746 p.
67. Chatfield, C., *The analysis of time series : an introduction*. 6th ed. Texts in statistical science. 2004, Boca Raton, FL: Chapman & Hall/CRC. xiii, 333 p.
68. *Cross-correlation Analysis of Filtered and Rectified Waveforms*. SCRC Data Capture and Analysis Software Tutorials [cited 2010 March 22]; Available from: http://www.scrc.umanitoba.ca/doc/tutorial/T14_crosscorr_filtered_wfs.doc.
69. Yaffee, R.A. and M. McGee, *Introduction to time series analysis and forecasting : with applications in SAS and SPSS*. 2000, San Diego: Academic Press. xxv, 528 p.
70. Cohen, J., *A power primer.* Psychol Bull, 1992. **112**(1): p. 155-9.
71. Nakagawa, S. and I.C. Cuthill, *Effect size, confidence interval and statistical significance: a practical guide for biologists.* Biol Rev Camb Philos Soc, 2007. **82**(4): p. 591-605.
72. de Jong, W.C., et al., *A fully implantable telemetry system for the long-term measurement of habitual bone strain.* J Biomech. **43**(3): p. 587-91.
73. Al Nazer, R., et al., *Analysis of dynamic strains in tibia during human locomotion based on flexible multibody approach integrated with magnetic resonance imaging technique.* Multibody System Dynamics, 2008. **20**(4): p. 287-306.

Table 2 - Previous Tibial Strain Research [2]

	Principal Strain (μstrain)		Comparison	Strain Rate (μstrain/s)	
	Maximum	Minimum		Maximum	Minimum
Lanyon et al.	395	-434	±26%	-	-4000
Burr et al.	437	-544	11%	11,006	-7183
Milgrom et al.	840	-454	23%	3955	-3306
Milgrom et al.	394	-672	20%	4683	-3820
Al Nazer et al.	490	-588		3800	-4100

Appendix A

Informed Consent

Informed Consent

Study Title:
The effect of height on musculoskeletal injury while performing drop landings

Study Rationale
The purpose of this project is to apply current methods in musculoskeletal modeling to evaluate the risk of tibial stress fractures while performing drop jumps from various heights. This information will be helpful in determining what causes stress fracture injuries in the lower limb in runners and other active people.

Inclusion Criteria

- Males between the ages of 18 – 27
- Body mass index of 28 or less
- Participate in recreational sport or exercise at least three times per week
- Free of any musculoskeletal injury
- Be classified as "low risk" as defined by ACSM's Guidelines for Exercise Testing and Prescription
- Must have CT scan done on both tibiae in the past 4 months.

Participation Periods and Duration

For this study you will participate in one session lasting less than an hour. During this session you will participate in the drop-landing data collection. The collection consists of 3 drop-landings from 3 different heights for a total of 9 trials. The three heights are taken from a previous study. You will perform drop-landings from 26, 39, and 52 cm (approximately 10, 15, and 20.5 inches). You will have a similar marker and EMG electrode attachment as the previous study in the Biomechanics Laboratory. You will be landing on to two force plates.

You have previously had a CT scan performed on your tibia. This data will be used for this study but will not require any additional time from you.

Data Confidentiality

The data collected during this study will remain confidential. You will not be identified in any way in subsequent publication or presentation of this research. Only members of the research team will have access to the data. Electronic data will be stored indefinitely on password protected computers in the Biomechanics Lab.

Associated Risk

There is minimal risk of injury during landing from a jump. Although it is unlikely, during drop-landing, you may lose balance and fall. However, a research staff will stand next to you and provide you with adequate support and protection.

Emergency Care

It is understood that in the unlikely event of an injury or illness of any kind as a result of your participation in this research project that Ball State University, its agents and employees will assume whatever responsibility is required by law. In the event that you should require it, emergency care will be provided to you at your expense. If any injury or illness occurs in the course of your participation in this research project, please notify Henry Wang or Scott Dueball at the BSU Biomechanics Laboratory, 765/285-5178.

Participation

Your participation in this study is completely voluntary. You are free to withdraw your permission at anytime for any reason without penalty or prejudice from any member of the research team. There is no direct and intended benefit to you. The only incentive to you is the participation in advanced scientific research and the knowledge that will be

gained by conducting such research. Please feel free to ask questions to clarify any of this form before signing it.

Consent

I, _____, agree to participate in this study, "The effect of height on musculoskeletal injury while performing drop landings." I have had the study explained to me and my questions have been answered to my satisfaction. I have read the description and give my consent to participate. I give my consent to use my CT scan data from previous studies for the current study. I understand that I can withdraw my consent at any time during the study if I feel uncomfortable. I understand that I will receive a copy of this informed consent form for my own reference.

I understand that my participation in this study depends on my responses given on the Intake Questionnaire and that I may not be selected if I do not meet the necessary criteria. To the best of my knowledge, I meet the inclusion/exclusion criteria for participation in this study.

_____
Participant's Name

_____ _____
Participant's Signature Date

_____ _____
Investigator's Signature Date

Principal Investigators

Scott S. Dueball
Ball State University
Biomechanics Laboratory
McKinley Avenue, PL 204
Muncie, IN 47306
847/946-2177
E-mail: ssdueball@bsu.edu

Henry Wang, Ph.D.
Ball State University
Biomechanics Laboratory
McKinley Avenue, PL 203
Muncie, IN 47306
765/285-5126
E-mail: hwang2@bsu.edu

For questions about your rights as a research subject, please contact:

Research Compliance
Sponsored Programs Office
Ball State University
Muncie, IN 47306
(765) 285-5070
E-mail: irb@bsu.edu

Appendix B

Software Descriptions

Workstation- Collection Software used to capture motion, force, and EMG data.

Visual 3D- C3D Post-Processing software. Marker and force data were filtered using this program. EMG data were also prepared for statistical analysis here.

MD Adams- Multibody Dynamics platform. Adams creates a 3-dimensional mechanical simulation for engineering tests. This is used extensively in the automotive industry to simulate mechanical parts working together. See LifeMOD for how this was used.

Mimics- Medical image processing software. CT Scans were used to create tibia geometry. Bone is highlighted on each slice to create a 3D object. The 3D Object is brought into Marc for further processing.

MD Marc/Mentat- Finite Element Analysis solver. Marc was used for the modal analysis on the tibia. Muscles and joints were created and attached to the tibial mesh using RBE2 links. The MNF produced in Marc was read directly into Adams (LifeMOD).

LifeMOD- Musculoskeletal modeling software. Motion, force, and flexible bodies were all used to create the movement simulation.